Characterization of cytosolic phosphoglucoisomerase (cPGI) through analysis of *Arabidopsis thaliana* mutants

Inaugural-Dissertation

zur

Erlangung des Doktorgrades

der Mathematisch-Naturwissenschaftlichen Fakultät

der Universität zu Köln

vorgelegt von

Shirin Zamani-Nour

aus Shiraz, Iran

Köln, 2014

Die dieser Dissertation zugrunde liegenden experimentellen Arbeiten wurden in der Zeit vom November 2010 bis June 2014 am Botanischen Institut der Universität zu Köln angefertigt.

Berichterstatter:	Prof. Dr. Ulf-Ingo Flügge
	Prof. Dr. Stanislav Kopriva

Tag der mündlichen Prüfung: 24.06.2014

“Don't be satisfied with stories, how things have gone with others. Unfold your own myth”

-- Rumi, Persian poet

TO MY PARENTS

Table of Contents

1. Introduction

1.1 Primary carbohydrate metabolism in plants

1.1.1 Starch and sucrose as carbohydrate storage and transport forms

A well-balanced carbohydrate metabolism is vital for all developmental stages during a plant's life cycle. Although the energy content of carbohydrates is approximately only half of that of lipids (Baud and Lepiniec, 2009), any perturbation of enzyme activity in either their biosynthesis or hydrolysis can have a major impact on plant performance. Starch and sucrose are the most important forms of stored and transportable energy. However, they also serve as substrates in multiple other pathways like amino acid, fatty acid, and cell wall constituent biosynthesis (Stitt and Zeeman, 2012) or regulation of growth and development together with gene expression (Dalchau et al., 2011). Moreover, their effects on flowering (Bernier et al., 1993; Levy and Dean, 1998), gametophyte development and seed maturation (Egli et al., 2010), nutrient deficiency (Liu and Vance, 2010), chilling tolerance (Sicher, 2011), plant productivity and yield (Gibson et al., 2011) have been well studied. It is known that the starch and sucrose biosynthesis pathways are closely related to each other. More than half of the carbon assimilated in chloroplasts will eventually be stored in transitory starch (Scialdone et al., 2013). On the other hand, starch degradation at night is important to supply sufficient amounts of carbohydrates for sucrose biosynthesis and respiration (Zeeman et al., 2004). Moreover, sucrose produced in mesophyll cells (palisade parenchyma) can be transported via the phloem to other plant parts (Chen et al., 2012). Investigating carbohydrate metabolism by characterizing key enzymes involved in carbohydrate turnover can help to better understand the importance of individual steps for the completion of a plant's life cycle but also the flexibility by which plants are able to compensate perturbations.

Plants are using photosynthesis to convert light energy into chemical energy in the form of sugars. This process exclusively takes place in chloroplasts of green tissues.

During the day two main processes are using the fixed carbon from photosynthesis. In the stroma of chloroplasts assimilated carbon is used for synthesis of transitory starch which is continuously accumulating over the course of the day. At the same time, fixed carbon as triose-phosphates (TP) exported from chloroplasts by triose-phosphate/phosphate translocator (TPT) is being used for the synthesis of sucrose in the cytosol (Smith et al., 2005). This sucrose serves as the major transport form of assimilated carbon from source to sink tissues.

Transitory starch in chloroplasts is used as energy storage for the coming night period to sustain metabolism and plant growth and provide substrates for sucrose synthesis while the photosynthetic machinery is inactive (Lloyd et al., 2005; Lu et., 2005). In Arabidopsis, the rate of transitory starch synthesis and degradation is rather linear (Scialdone et al., 2013; Figure 1). Starch content in leaves is steadily increasing over the course of the day. With the onset of the dark period starch is gradually degraded until about 95% of starch have been broken down and utilized by the end of the night (Figure 1; Yazdanbakhsh et al., 2011; Scialdone et al., 2013). Environmental conditions such as the day length, light intensity and temperature affect starch turnover which means for example that in long-day conditions nocturnal starch breakdown proceeds faster than in short-day conditions (Seaton et al., 2014; Figure 1). Hence, adjustment of starch metabolism enables continuous growth along with decreasing the risk of carbon starvation (Sulpice et al., 2014). Therefore, any manipulation of carbohydrate turnover by impairing either sucrose or starch biosynthesis will hamper carbon flux and metabolism and further impact plant growth and development.

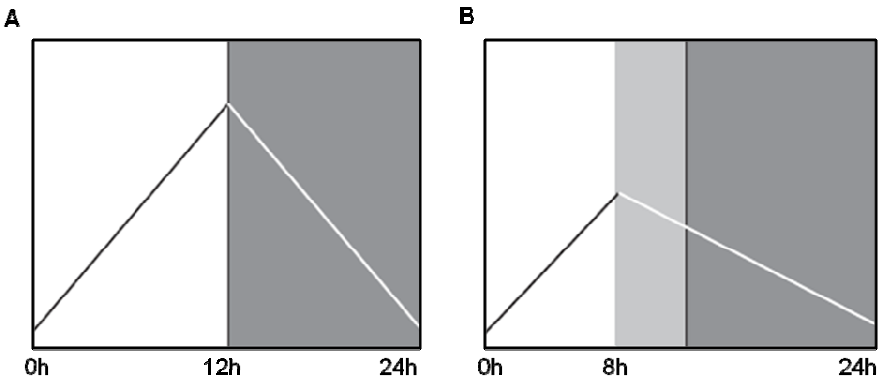

Figure 1: The linear trend of starch degradation and its adaptation to the night length in *Arabidopsis thaliana* (A) *A. thaliana* grown in 12 h/12 h light/night cycle (B) *A. thaliana* grown in 8 h/16 h light/night cycle. The dark shades are the 12 h darkness and the light shade is when plant placed unexpectedly to an early night (Adapted from Graf and Smith, 2011).

1.1.2 Hexose-phosphate pools as hubs of carbohydrate metabolism

Starch biosynthesis in the stroma of plastids and sucrose production in the cytosol are important metabolic pathways to regulate the carbon skeleton partitioning needed for plant growth and development and therefore, these pathways potentially rely on the appropriate maintenance of hexose phosphate pools as substrates in the stroma and the cytosol. In other words, generation and turnover of starch and sucrose are closely linked to the existence of pools of phosphorylated, i.e. metabolically activated hexoses. Two spatially separated hexose phosphate pools can be found in plant cells – one in plastids and one in the cytosol. Both pools comprise fructose-6-phosphate (Fru6P), glucose-6-phosphate (Glc6P) and glucose-1-phosphate (Glc1P) but serve different purposes.

In chloroplasts hexose phosphates are the starting points for starch biosynthesis. Here, Glc6P is generated from the primary photosynthetic product Fru6P by plastidic phosphoglucoisomerase (PGI1) and can be further converted to Glc1P by action of phosphoglucomutase (PGM). Glc1P serves as substrate for ADP-glucose pyrophosphorylase (AGPase) which catalyzes the generation of ADP-glucose, the primary substrate of starch synthesis (Stitt and Zeeman, 2012). The final step of starch biosynthesis is mediated by the complex of starch synthases that transfer glucose moieties from ADP-glucose to the starch backbone. Loss-of-function mutants in any of the enzymes involved in starch biosynthesis are unable to produce transitory starch and referred to as starch-free mutants e.g. *pgi1-1* (Yu et al., 2000; Kunz et al., 2010), plastidic *pgm* (Caspar et al., 1985; Kofler et al., 2000) and *adg1-1* (Lin et al., 1988). However, some of these mutants may contain minor residual levels of starch. For example, lack of the PGI1 enzyme can be compensated in heterotrophic plastids by the Glc6P/phosphate translocator GPT leading to starch-containing plastids in root columella cells, stomata and bundle sheath cells (Kunz et al., 2010).

In contrast to chloroplasts, the cytosolic hexose phosphate pool feeds into diverse metabolic pathways such as glycolysis and respiration, synthesis of cell wall monomers and generation of sucrose. In the cytosol, interconversion of Glc6P and Fru6P which are key substrates for sucrose biosynthesis is carried out by cytosolic phosphoglucoisomerase (cPGI). Continuous production of sucrose is crucial for

plants throughout the day/night cycle. As such, generation of Fru6P as substrate for sucrose phosphate synthase (SPS) totally relies on cPGI activity at night, due to inactivated fructose 1,6-bisphosphatase, which is pivotal for sucrose production via the day path of carbon (Cseke et al., 1982; Stitt, 1990).

UDP-glucose, the other substrate for sucrose synthesis, is supplied by the sequential conversion of Fru6P, Glc6P and Glc1P via cPGI, cPGM and UDP-glucose pyrophosphorylase activity, respectively. Sucrose synthesis at night is fueled from transitory starch breakdown (Zeeman et al., 2007) and transport of its cleavage products (maltose and glucose) across the chloroplast membrane into the cytosol (Weber et al., 2000; Niittylä et al., 2004; Weise et al., 2004; Cho et al., 2011). Maltose exported from chloroplasts at night is integrated into cytosolic heteroglycans by disproportionating enzyme 2 (DPE2) in the cytosol (Chia et al., 2004; Lu and Sharkey, 2004), thereby releasing glucose into the cytosol (Fettke et al., 2005). DPE2-released as well as chloroplast-exported glucose can be converted by hexokinase to Glc6P and eventually to Glc1P and the glucose moieties of heteroglycans can be directly released as Glc1P by cytosolic glucan phosphorylase 2 (cPho2) (Fettke et al., 2004; Lu et al., 2006). Eventually, Glc1P is incorporated into UDP-glucose and sucrose production. Sucrose-phosphate synthase (SPS) and sucrose-phosphate phosphatase (SPP) are two enzymes which are needed for the last step of sucrose biosynthesis; the first enzyme converts the UDP-glucose together with Fru6P to sucrose 6P, UDP and H^+ and the second one converts sucrose phosphate (Suc-P) to sucrose.

The opposite reaction to sucrose synthesis, sucrose breakdown, is carried out by two different groups of enzymes, either the sucrose synthases which produce fructose and UDP-glucose or the invertases which produce Fru6P and Glc6P (Koch, 2004). However, only Fru6P is subjected to further glycolytic degradation and cPGI becomes important for conversion of Glc6P to Fru6P in glycolysis, the main energy supplier for heterotrophic tissues (Figure 2).

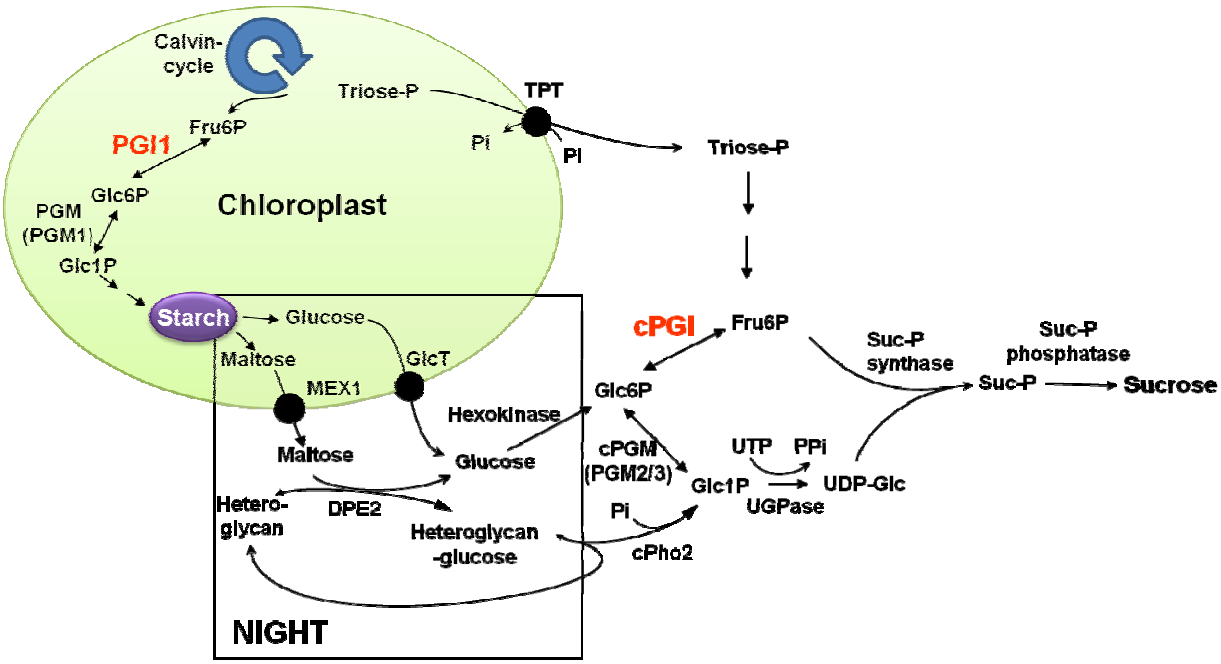

Figure 2: Schematic representation of carbohydrate metabolism in *Arabidopsis thaliana*

1.2 Cytosolic phosphoglucoisomerase – molecular weight, kinetics, and mutant analysis in Arabidopsis and other plant species

The PGI family is consisting of two different sub-families; the PGI and the bifunctional sub-family of phosphoglucose/phosphomannose isomerase (PGI/PMI) (Hansen et al., 2005). *Arabidopsis thaliana*'s PGIs (PGI1 and cPGI) belong to the PGI sub-family which are not only important for carbohydrate metabolism in plants but also all other forms of life that depend on carbohydrate breakdown via glycolysis. Two isoenzymes of the PGI were first reported in spinach leaves by Schnarrenberger and Oeser (1974) and later, the same results were obtained in *Arabidopsis thaliana* (Caspar et al., 1985), although some other plants like *Clarkia* (Gottlieb and Higgins, 1984) or *Arabidopsis halleri* (Kawabe et al., 2002) may have two *cPGI* loci due to a gene duplication (Gottlieb, 1977). The *cPGI* gene of *Arabidopsis thaliana* has been cloned and sequenced some 20 years ago (Thomas et al., 1993). The Arabidopsis cPGI has a molecular mass of 61.7 kDa (TAIR site: http://www.arabidopsis.org) which is in the range of 60-62 kDa reported for other species like spinach (Herbert and Schnarrenberger, 1982), *Clarkia xantiana* (Gottlieb and Higgins, 1984) and *Cassia coluteoides* (Lee and Matheson, 1984).

The protein sugar isomerase domain (SIS) can be found in different enzymes having the sugar phosphate isomerization activity. Hence, plant PGI is not an exception and consists of two α/β domains (Troncoso-Ponce et al., 2010). The biochemical characteristics of cPGI are rather conserved during evolution (Zhou and Cheng, 2008) and the kinetic characteristics of it have previously been determined in rabbit (muscle and brain), human (red blood cells) (Kahana et al., 1960) and wheat (endosperm) (Sangwan and Singh, 1989). According to the proteomic analysis, the K_m for Fru6P and Glc6P are 300 µM and 580 µM, respectively (Vosloh, 2011). The K_m values differed in different studies on different plants, e.g. in wheat endosperm, the K_m of 0.18 mM (Fru6P) and 0.44 mM (Glc6P) were obtained (Sangwan and Singh, 1989) and in spinach leaves, the K_m were 5.9 mM and 300 µM for Glc6P and Fru6P as substrates, respectively (Schnarrenberger and Oeser, 1974). The activities of cPGI enzymes are known to be affected by different inhibitors. In Arabidopsis, glycerol-3P could inhibit the total PGI activity (Quettier et al., 2008). In addition, Kahana et al. (1960) found out that ATP, Pi, PEP and 6-phosphogluconate are possible inhibitors of cPGI activity extracted from rabbit. On the other hand, in wheat endosperm, enzyme inhibitors of cPGI activity containing ribose-5P, ribulose-5P and 6-phosphogluconate were reported (Sangwan and Singh, 1989). Moreover, in spinach, cPGI activity was reduced to 49% using 5 mM Zn^{2+} (Weeden and Gottlieb, 1982) and in *Cassia*, besides 6-phosphogluconate, the enzyme was inhibited by erythrose-4P (Lee and Matheson, 1984). Interestingly, cPGI activity is known to be more heat resistant than the plastidic isoform which is inactivated at temperatures of 50-55°C (Weeden and Gottlieb, 1982; Zhu and Cheng, 2008).

In plants, investigation of impaired *cPGI* function has so far only been carried out through analysis of EMS-mutagenized *Clarkia xantiana* plants (Jones et al., 1986a; Kruckeberg et al., 1989; Neuhaus et al., 1989). *Clarkia* harbors two isoenzymes for cPGI and while each of the homozygous single mutants showed a dramatic reduction of cPGI activity, this was further reduced to 18% in the double mutant *cpgi2cpgi2/*cPGI3*cpgi3* (Jones et al., 1986a; Kruckeberg et al., 1989). The phenotypic properties of these mutants revealed a reduced sucrose biosynthesis and increased starch accumulation as results of reduced cPGI activity (Kruckeberg et al., 1989).

Besides, a loss-of-function mutant defective in a different enzyme involved in maintaining the cytosolic hexose phosphate pool has recently been characterized in

form of the *cpgm* mutant (Egli et al., 2010). In Arabidopsis, there is only one PGM located in plastids; however, in contrast to cPGI, there are two isoforms of PGM located in the cytosol (PGM2 and PGM3) (Caspar et al., 1985; Egli et al., 2010). Although homozygous T-DNA mutants in each single locus (*pgm2* or *pgm3*) were viable and grew normally, the double mutant *pgm2/pgm3* was lethal. This indicates that lack of one isoform could be compensated by the other one (Egli et al., 2010).
The plastidic isoform of PGI (PGI1), as previously described, is essential for transitory starch synthesis in chloroplasts and its loss-of-function mutant (*pgi1-1*) is virtually starch-free but viable (Yu et al., 2000). In contrast, no information is available about the physiological phenotypes of loss-of-function mutants in *cPGI* and impairment of its function has so far not been investigated in *Arabidopsis thaliana.*

1.3 Aim of current study

This study was conceived to investigate the global role of cPGI in metabolism using the model organism *Arabidopsis thaliana*. To this end, analyses of T-DNA insertion mutants and artificial micro RNA knock-down mutants were performed to determine the degree of functional essentiality of cPGI. In addition, complementation of heterozygous *cpgi* mutants by *cPGI* overexpression using ubiquitous or developmental stage-specific promoters were intended to identify phases where cPGI activity is particularly critical.
Moreover, thorough metabolite analysis in plants with decreased or absent cPGI activity aimed at the question of functional redundancy and metabolic flexibility in plants having to cope with the inability to properly maintain cytosolic hexose phosphate pools via action of cytosolic phosphoglucoseisomerase. Results from these investigation were anticipated to extent our knowledge not only on cPGI importance but also on strategies employed by plants to persist in situations of metabolic imbalance.

2. Materials and Methods

2.1 Plants

2.1.1 Plant materials

Arabidopsis thaliana ecotype Wassilewskija (Ws) was used as wild-type control for *dpe2* mutants, for all other experiments *Arabidopsis thaliana* ecotype Columbia (Col-0) was used as a wild-type control. Mutant alleles of *pgi1-1* (Yu et al., 2000) and *adg1-1* (Lin et al., 1988) were used either as a starch-free negative control or for preparation of double mutants. Both T-DNA lines of *cPGI*; *cpgi-1* (Salk_064423) and *cpgi-2* (Salk_016862) were ordered from the Nottingham Arabidopsis Stock Center (NASC) (Alonso et al., 2003). Genotyping to identify homozygous individuals from annotated homozygous (*cpgi-1*, Salk_064423) or segregating heterozygous (*cpgi-2*, Salk_016862) T-DNA lines were carried out using primers: cPGI fwd5, cPGI rev 10 and Salk left border primer LBaI (for sequences see 2.12). No homozygous individuals could be identified for *cpgi-1* or *cpgi-2.* The T-DNA insertion lines *fum2-1* (SALK_025631) and *fum2-2* (GABI_107E05) (Pracharoenwattana et al., 2010; Brotman et al., 2011) were ordered from the Arabidopsis Biological Resource Center. The unpublished line *fum2-3* (SALK_149466) was provided by Junshi Yazaki (The Salk Institute, La Jolla). Homozygous mutants for all three lines were isolated using primers: FUM2 fwd3, rev5 and Salk left border primer LBaI or GABI LB, respectively (for sequences see 2.12). The *dpe2* lines (Lu and Sharkey, 2004) were provided by Thomas Sharkey (University of Wisconsin, Madison).
Moreover, for all experiments involving amiRNA, the amiRNA1 lines (*6* and *10*) were selected from a segregating T3 population and the amiRNA2 lines (*8*, *9* and *10*) were selected from a segregating T2 population based on occurrence of the high NPQ phenotype.

2.1.2 Accession numbers

Sequences of all loci investigated can be found in publicly available Arabidopsis data bases according to their AGI code: *PGI1* (At4g24620), *cPGI* (At5g42740), *ADG1* (At5g48300), *FUM2* (At5g50950) and *DPE2* (At2g40840).

2.1.3 Growth conditions

In vitro culture was performed on ½ strength Murashige-Skoog medium. The pH was adjusted to 5.6-5.8/KOH and medium was autoclaved. Seeds were stratified for two days at 4°C. Afterwards, plates were placed in a growth chamber under the temperature of 22°C day /20°C night and 60% humidity. Normally, 11 days after germination, small seedlings were transferred to the soil and placed in the growth chamber. Depending on the experiment, plants were cultivated either in long-day condition (16 h day/8 h night) or short-day condition (8 h day/16 h night) or sometimes transferred to the greenhouse which is running at long-day condition with the temperature of 22°C day /18°C night and 40% humidity.

½ Strength Murashige-Skoog (MS) Medium

0.22% (w/v)	MS salts including modified vitamins (Duchefa, Haarlem, NL)
0.5 - 2% (w/v)	Sucrose
0.8% (w/v)	Phyto-Agar (Difco)

2.1.4 Dry sterilization of seeds

Seeds were surface sterilized under the clean bench by incubation in 1 ml of 70% EtOH in an Eppendorf tube for 5 min and centrifuged at 14,000 rpm for a few seconds. The ethanolic supernatant was discarded and 100% EtOH was added. The Eppendorf tubes were then vortexed for a few seconds and after removal of the ethanolic supernatant in the Eppendorf tube in the stream of sterile air under the clean bench, dry seeds were dispersed evenly on the medium.

2.1.5 Leaf area and fresh weight determination

For leaf fresh weight measurement, 3- and 4-week-old plants (long-day condition) or 4- and 5 week-old plants (short-day condition) in individual pots were first photographed and then whole rosettes were weighed. The leaf area was calculated from images utilizing the software ImageJ 1.47m (http://imagej.nih.gov/ij/).

2.2 Microbial methods

2.2.1 *Escherichia coli* (*E. coli*) bacteria growth condition

The bacteria strain of DH5a with the chromosomal genotype of *fhuA2 lac(del)U169 phoA glnV44 Φ80' lacZ(del)M15 gyrA96 recA1 relA1 endA1 thi-1 hsdR17* was used in all cloning procedures. *E. coli* bacteria were grown in either liquid LB (Luria Betani) culture with the appropriate antibiotic in an orbital shaker at 37°C, 220 rpm or on LB plates at 37°C in the oven. Glycerol stocks of clones were stored at -80°C in LB with 50% glycerol.

LB Medium

1% (w/v)	Trypton
0.5% (w/v)	Yeast extract
1% (w/v)	NaCl
1.5% (w/v)	Bacto agar (only used for the plate)

Autoclaved

2.2.1.2 Preparation of *E. coli* competent cells

For preparation of *E. coli* competent cells, 2 µl of *E. coli* cells were added to 10 ml Ψb medium as a pre-culture and incubated over night at 37°C in 220 rpm orbital shaker. At the same time, 400 ml of Ψb medium in 1000 ml Erlenmeyer flask were placed in shaker at 37°C. On the following day, 4 ml of the pre-culture were diluted into the 400 ml of pre-warmed medium. The culture was then incubated shaking at

37°C until an OD_{600} of 0.48 was reached (about 2-2.5 h). After this point, the culture was incubated on ice for 15 min and subsequently, cells were sedimented at 2,000 rpm for 10 min at 4°C. Supernatants were discarded and the pellets were resuspended gently in 1 ml TFB1 buffer. From this step further on, all work was done at 4°C. After 2 h of incubation on ice, cells were spun down at 2,000 rpm for 5 min at 4°C. Finally, cell pellets were resuspended in 2 ml of TFB2 buffer, aliquoted at 100 µl in pre-cooled 1.5 ml Eppendorf tubes, frozen in liquid nitrogen and stored at -80°C.

Ψb Medium (500 ml)

10 g	Bacto trypton
2.5 g	Bacto yeast extract
2 g	$MgSO_4.7H_2O$ (4%)
0.375 g	KCl (10 mM)

pH was a adjusted to 7.6 by 1M KOH

Autoclaved

TFB1 buffer (100 ml)

1.21 g	$RbCl_2$ (100 mM)
0.99 g	$MnCl_2.4H_2O$ (50 mM)
0.3 g	KOAc (30 mM)
0.15 g	$CaCl_2.2H_2O$ (10 mM)
100%	Glycerol (15% v/v)

pH was adjusted to 5.8 by acetic acid

TFB2 buffer (20 ml)

0.0242 g	$RbCl_2$ (10 mM)
0.2205 g	$CaCl_2.2H_2O$ (75 mM)
0.0419 g	MOPS (10 mM)
100%	Glycerol (15 % v/v)

pH was adjusted to 7 by 1M or 0.5 M NaOH

TFB1 and TFB2 were filter-sterilized

2.2.2 *Agrobacterium tumefaciens* growth condition

Different Agrobacterium strains were used including GV3101 and GV3101 (pMP90RK). Agrobacteria were grown in either the liquid YEB culture with the appropriate antibiotics (see 2.11) at 28°C in the 220 rpm orbital shaker or on solid YEB plates at 28°C in the oven. Stock cultures of positive clones were stored at -80°C in YEB supplemented with 50% glycerol.

YEB Liquid medium

5 g Bacto pepton
5 g Beef extract
1 g Yeast extract
5 g Sucrose
0.5 g $MgSO_4.7H_2O$
1 L H_2O_{dd}
1.5% Bacto agar (only used for the plate)
Autoclaved

2.2.2.1 Preparation of *Agrobacterium tumefaciens* competent cells

For preparation of competent Agrobacterium cells, 50 µl of Agrobacterium cells were incubated as a pre-culture in 20 ml YEB medium with antibiotics appropriate for the particular Agrobacterium strain (see 2.11) and incubated for 2 days at 28°C in an orbital shaker. Then an appropriate volume of the pre-culture was diluted into 1000 ml YEB medium to give an OD_{600} of 0.033. The antibiotic Rifamycin (20 µg/ml) was used for all agrobacteria strains in the main culture. The culture was then continuously incubated for about 10 h to reach an OD_{600} of 0.5-0.6. The culture was then kept on ice for 5 min, centrifuged at 4,000 rpm for 15 min at 4°C, resuspended in 5 ml of pre-cooled NaCl (150 mM) and incubated for another 15 min on ice. After another centrifugation at 4,000 rpm for 5 min at 4°C, the pellet was resuspended in 2 ml of pre-cooled 20 mM $CaCl_2$. Finally, 50 µl aliquots were prepared in 1.5 ml pre-cooled Eppendorf tubes and stored at -80°C.

2.3 Molecular biological methods

2.3.1 Genomic DNA isolation

Genomic DNA was isolated from a single leaves. One leaf was ground in a 1.5 ml Eppendorf tube with pestle. Then, leaf material was incubated in 500 µl of extraction buffer (EB). Afterward, tubes were centrifuged at 14,000 rpm for 5 min and the supernatant was transferred to a new tube. For about 450 µl of supernatant, 450 µl isopropanol was added and mixed well. After 10 min of incubation at room temperature, samples were centrifuged at 14,000 rpm for 10 min. The supernatant was removed and the pellet washed 2 times with 70% ethanol. The dries DNA pellet was resuspended in a volume of sterile water (H_2O_{dd}) that depended on the leaf size (50-200 µl) and stored in -20°C. To increase the DNA purity, the pellet was resuspended after the precipitation with isopropanol in 450 µl of TE buffer. After centrifugation for 3-5 min at full speed, about 400 µl of solution were transferred to a new tube and genomic DNA was precipitated by addition of 40 µl of 3 M sodium acetate (NaOAc) and 1 ml of 100% pre-cooled ethanol and kept at -20°C for at least 10 min. After centrifugation for 10 min, the pellet was washed 2 times with cold 70% ethanol and let to be dried completely before resuspension in H_2O_{dd}.

EB Buffer		**TE Buffer**	
200 mM	Tris, pH 7.5/HCL	10 mM	Tris, pH 8.0
250 mM	NaCl	1 mM	EDTA
25 mM	EDTA		
0.5%	SDS		

2.3.2 Plasmid DNA purification (Miniprep)

Plasmid DNA was extracted from a 5 ml over night culture with the help of the Quantum Prep Plasmid Mini Kit (BioRad München, D). The first three solutions of the kit including cell resuspension, cell lysis and neutralization were used, but instead of the DNA binding matrix, plasmid DNA was precipitated using 800 µl isopropanol.

After centrifugation for 10 min at 14,000 rpm, plasmid DNA was dissolved in 50 µl of distilled water.

2.3.3 RNA extraction

Prior to RNA extraction, the Eppendorf tubes and centrifuge were pre-cooled down to 4°C. For RNA extraction, 50-100 mg Arabidopsis leaf material homogenized using liquid nitrogen. Then, 1 ml Z6 buffer was added. The homogenized sample further transferred to 2 ml Eppendorf tube and 500 µl phenol/chloroform/isoamyl alcohol in a ratio of 25:24:1 was added. After shaking and centrifugation at 20,000 g for 15 min, the supernatant was transferred to a new tube and mixed with 1/20 volume 1 M acetic acid and 0.7 volume 100% ethanol for RNA precipitation and centrifuged for 10 min. The supernatant was removed and then, the pellet was washed two times consequently with 500 µl 3 M Na-acetate (pH 5.0) and with 500 µl of 75% ethanol by simply converting the tube. After another centrifugation at 20,000 g for 15 min, the pellet was dried out at room temperature and resuspended at RNAse free water. Finally, the RNA was stored at -20°C.

RNA quality was tested using agarose gel electrophoresis by mixing 1 µl of RNA sample with 10 µl $H2O_{dd}$ and 4 µl of loading buffer using 1.2% agarose gel. Occurrence of 2 bands from rRNA is an indicator for the good RNA quality that could be used for future cDNA synthesis.

Z6 buffer

8 M	Guanidine hydrochloride
20 mM	MES pH 7.0
20 mM	EDTA

2.3.4 cDNA synthesis

For cDNA synthesis, extracted RNA was used as template for reverse transcriptase to synthesize the single strand cDNA.

2.3.4.1 DNAse reaction

To reach the high purification level of RNA and avoid of any DNA contamination, DNAse treatment was performed. For this approach, 2 µg RNA were incubated with 1.5 µl 10x DNAse buffer and 1 µl DNAse I (Ambion) in a total volume of 20 µL for 60 min at 37°C. The 2 µl of inactivation substance was added and incubated for 2 min at room temperature. After centrifugation at 10,000 g for 1 min, the 10 µl of supernatant was used for the following reverse transcription reaction.

2.3.4.2 Reverse transcription (RT)

For RT reaction, 10 µl of final samples from previous step (2.3.4.1) was incubated with 1 µl oligo dTs (0.5 µg/µl) and 1 µl RNAse free water for 5 min at 70 °C coupled with 3 min on ice. Afterwards, 0.25 µl Bioscript (200 U/µl, Bioline), 1 µl dNTPs (10mM), 4µl 5x Bioline buffer and 2.75 µl RNAse free water were added to the solution to get the total volume of 20 µl. The sample was briefly vortexed and placed at 37°C. Finally, the sample was incubated at 70°C for 10 min for stopping the reaction and stored at -20°C for further experiments.
The quality of synthesized cDNA was tested via PCR together with gel electrophoresis using actinI (house-keeping gene) specific primer pairs (for sequence see 2.12).

2.3.5 Determination of the nuclear /plasmid DNA concentration

DNA concentration was determined by adding 1 µl of sample using the Nanodrop ND-1000 (Peqlab) photometer at a wavelength of 260 nm. In the case of plasmid DNA determination, the recorded number of 1.80-1.90 at the wavelength ratio of A260/280 is an indicator for the least contamination with RNA and the number around 2 at the wavelength of A260/230 indicates a pure plasmid DNA without protein contamination.

2.3.6 DNA sequencing

DNA sequencing was performed for either the direct PCR product for finding the position of inserted T-DNA or the plasmid vector for checking the correct insertion of gene of interest without any misreading or mutation. The reaction was carried out in a thermo-cycler MJ Research PTC-200 Peltier Thermal Cycler (BioRad, München, D) using the Big Dye Terminator v3.1 cycle sequencing kit (Applied Biosystems Austin, TX, USA). The further detection was obtained by ABI 3730 Genetic Analyzer (PE Applied Biosystems GmbH) in the Institute of Genetics of the University of Cologne.

Sequencing mixture

2.25 µl	5x Big Dye sequencing buffer
0.25 µl	primer (10 µmol/µl)
0.25 µl	Big Dye v3.1
10-100 ng/100bp	DNA templates

Adjusted with H_2O_{dd} to a total volume of 10 µl

Sequencing programme

1) Denaturation	96°C 2 sec
2) Denaturation	96°C 10 sec
3) Annealing	55°C 10 sec
4) Elongation	60°C 4 min
5) 4 °C forever	Steps 2-4 were repeated 30 times

2.3.7 Polymerase Chain Reaction (PCR) for genotyping

To distinguish homozygous from heterozygous plants, two different primer (oligonucleotides) combinations were used. One combination was the genome specific primers and another combination was the primer which has been designed from left border (LB) of T-DNA together with sense or antisense of genomic DNA depending on previous determination of T-DNA insertion site. Homozygosity then can be identified by gel electrophoresis of PCR products (1% agarose gel; agarose

in 1% TAE solution buffer). Having no band with the first primer combination and occurrence of a band with the second primer combination is an indicator for the presence of T-DNA in both homologous chromosomes and homozygosity.

Standard PCR master mix

15.95 µl	H_2Odd (up to 20 µl)
2 µl	10x Dream Tag Green Buffer (1/10 vol.)
0.2 µl	dntps (dATP,dGTP,dCTP,dTTP) (100 µM)
0.4 µl	forward primer (10 pmol/µl, 1/50 vol.)
0.4 µl	reverse primer (10 pmol/µl, 1/50 vol.)
0.05 µl	Dream Taq-Polymerase (1U)
1 µl	DNA template (1-100 ng)

For cloning purposes, the proof-reading Pfu-polymerase (Thermo Scientific, Fermentas) and the Pfu-buffer containing MgSO were used.

PCR program was used in a thermo-cycler MJ research PTC-200 Peltier Thermal Cycler (Biorad, München, D).

PCR program in thermo cycler

1- Denaturation	95-98 ºC	5 min
2- Denaturation	95-98 ºC	30 sec
3- Annealing	55 ºC	30 sec
4- Elongation	72 ºC	1 min
5- Elongation	72 ºC	10 min
6- Constant temperature	16 ºC	forever

Steps 2-4 were repeated for 30 times.

2.3.7.1 Colony PCR of *E. coli* colonies

In many cases, colony PCR was performed by picking a single colony using a sterile pipette tip and transferring adhering cells into a PCR standard master mix. In the case that PCR did not work, the colony was swirled into 25 µl 1xTE buffer or H_2O_{dd}

and heated for 2 min in water bath at 90°C. One microliter of that solution could alternatively be used as PCR template either directly or after centrifugation.

TE Buffer

10 mM Tris, pH 8.0
1 mM EDTA

2.3.7.2 Colony PCR of Agrobacterium colonies

Since agrobacteria cell walls are harder than *E. coli* and it is harder to get the plasmid DNA out of the cells, a single colony was picked using a pipette tip, swirled in 0.02 M NAOH and heated in a water bath to 90°C for 10 min. After a short centrifugation, 1 µl of the supernatant was added as template into a standard PCR mix.

2.3.8 Agarose Gel-Electrophoresis

Horizontal agarose gel electrophoresis was used to separate DNA fragments according to their size and charge. One percent (w/v) of agarose was suspended in TAE buffer heated in a microwave until becoming completely dissolved. Ethidium bromide was added to interact with DNA molecules and make it visible under UV light. The whole mixture was poured in the electrophoresis chamber with the comb. After solidification, the comb was removed and each PCR product was pipetted into a separate well. Since Dream Tag green buffer was used, there was no loading buffer needed to load the DNA on the gel, otherwise 10x loading buffer was needed. Depending on the gel size, 80 or 150 V (const.) was used for electrophoresis.

50x Tris/Acetate Buffer (TAE)

2 M Tris/HAc, pH 7.5
50 mM EDTA

2.3.9 DNA elution from agarose gel

For cloning procedure, DNA is needed to be eluted from agarose gel. For this purpose, the separated DNA on agarose gel under the UV-table with protection was quickly separated and placed into the Eppendorf tube. Subsequently, the elution steps were finalized using the Ultra-Sep Gel Extraction Kit (Omega bio-tek, Norcross, GA, USA) according to the manufacturer's instructions.

2.3.10 Restriction enzyme digestion

For generation of specific sticky ends on DNA/vector, the restriction digestion was performed utilizing enzymes from Thermo Scientific (Fermentas) and used according to the manufacturer's instructions. The restriction enzymes could further cleave the specific parts of DNA/vector according to their recognition sites.

2.3.11 DNA dephosphorylation

A day after restriction digestion and prior to ligation step, the digested vector plasmid was dephosphorylated using 1 µl of SAP (Thermo Scientific, Fermentas) to avoid of probable religation of vector. The samples were kept for 1 h at room temperature before starting the next step.

2.3.12 DNA ligation

During cloning procedure and for ligation of specific DNA fragment into the plasmid vector, a T4 DNA ligase (5 U/µl, Thermo Scientific, Fermentas) and 1xT4 ligase buffer were used according to the manufacturer's instructions with the total volume of 10 µl. The T4 ligase links the 3'-OH and 5'-phosphate group which is coupled with ATP hydrolysis. Samples were further incubated over night at 20°C before used for the next step.

2.3.13 L/R reaction

The L/R reaction is a step in Gateway cloning system based on homologous recombination for which, DNA fragment can be inserted first between attL-sites in the pENTRY vector backbone (using classical restriction enzyme digestion or TOPO reaction) and subsequently transferred between the attR-sites in any destination vectors of interest (using L/R reaction). The L/R reaction is conducted using L/R clonase (Life technologies, Invitrogen) and incubated over night at room temperature. The products yielded from L/R reaction were finally transformed into bacteria DH5a cells for more amplification.

LR-reaction

30 ng	Entry clone
30 ng	Destination vector
0.2-0.4	LR clonase enzyme mix
Up to 2 µl	$H2O_{dd}$

2.3.14 TOPO reaction

The blunt end PCR products can be easily inserted into the gateway compatible pENTR/D-TOPO vector (Invitrogen, Carlsbad,CA, USA) through TOPO reaction. For this purpose, the pENTR/D-TOPO Cloning Kit (Invitrogen, Carlsbad, CA, USA) were used according to the manufacturer's instructions.

2.3.15 Cloning

2.3.15.1 Cloning of *PGI* and *cPGI* open reading frames

The open reading frame of the two isoenzymes PGI and cPGI were amplified using complementary DNA (cDNA), reverse transcribed from total RNA extracted from Arabidopsis leaf material. The cDNAs without stop codon were amplified with restriction sites of XbaI/XmaI and BamHI/XmaI for *PGI1* and *cPGI*, respectively and

cloned into the vector pJet1.2 (Thermo Scientific Life Science). After sequencing to check for accuracy of the sequences, the cDNA was subsequently transferred to either SpeI/XmaI (*PGI1*) or BamHI/XmaI (*cPGI*) opened pUBQ10:pHygII-UT-c-term-Venus to shape the final expression vectors (Norris et al., 1993; Krebs et al., 2012). The pUBQ10:pHygII-UT-c-term-Venus vector has a mutation in SacI restriction site-MCS-Venus-HSP18.2 terminator (Nagaya et al., 2010). The construct was developed by Rainer Waadt and cloned via HindIII/EcoRI into hygII-MCS plasmid (Walter et al., (2004), provided by Jörg Kudla's laboratory, Wetsälische Wilhelms Universität Münster /Germany).

2.3.15.2 Cloning of artificial microRNA (amiR)

The two cPGI amiRNA lines (amiRNA1: TGTACTGTTAATATGCTCCCG and amiRNA2: TATCTAGAACGTTCCAGACTT) were generated using specific primers designed for the amiRNA stem sequence (see 2.12) with the online tool at http://wmd3.weigelworld.org (Schwab et al., 2006). The TOPO- and Gateway cloning system (Life Technologies) were used to generate the p35S: amiRNA lines. Entry vectors (pENTR/D-TOPO vector) harboring *cPGI* specific amiRNAs were generated using PCR products according to the manufacturer's instructions and after verifying amiRNA sequence faultlessness, they were transferred through L/R reactions to the destination vector pGWB2 (Nakagawa et al., 2007). Expression vectors were transformed into *Agrobacterium tumefaciens* GV3101 which were used for plant transformation.

2.3.15.3 Cloning of complementation constructs

Except the pUBQ10 construct that was classically cloned (2.3.15.1), for the rest of complemented lines (p35S and pUSP), the gateway compatible pENTR/D-TOPO (Invitrogen, Carlsbad) was used for primary cloning of *cPGI* cDNA for amplification in *E. coli* DH5a. The *cPGI* cDNA was amplified by PCR and cloned into pENTR/D-TOPO. The sequence-verified *cPGI* cDNA was transferred via L/R-recombination reaction to destination vectors p35S_pAMPAT and pUSP_pAMPAT to yield

p35S::cPGI and pUSP::cPGI complementation constructs. In addition, the previously described expression vector pUBQ10::cPGI::pHygII-UT-c-term-Venus (see 2.3.9.1) was also used for complementation analysis. pUBQ10::cPGI::pHygII-UT-c-term-Venus was transferred into *Agrobacterium tumefaciens* strain GV3101 and p35S/pUSP::cPGI::pAMPAT vectors were transferred to *Agrobacterium tumefaciens* strain GV3101 pMP90 RK.

Destination vector	**Promoter in vector backbone**
p35_pAMPAT	35S cauliflower mosaic virus (CaMV)
pUSP_pAMPAT	Unknown Seed promoter (USP)
pHygII-UT-c-term-Venus	Ubiquitin-10 gene promoter (UBQ10)

2.4 Metabolite measurements

2.4.1 Sucrose, starch and heteroglycans measurements

Sucrose and starch measurements can be performed right after each other from the same plant materials. For this approach, 900 µl of 80% ethanol was added to 80-100 mg of ground, frozen leaf material and incubated for 1 h at 75°C. After centrifugation for 5 min at 14,000 rpm, 500 µl of the supernatant were transferred to new Eppendorf tubes for sucrose measurement and placed in a centrifugal evaporator (SpeedVac/Eppendorf, Concentrator 5301) for the complete evaporation of ethanolic supernatant at room temperature. Dried extracts were resuspended in 500 µl $H2O_{dd}$ using an enzyme spatula. After a 5 min centrifugation at 14,000 rpm, 10 µl of the sample were added to 190 µl solution of 100 µl H_2O_{dd} and 90 µl assay buffer prepared for photometric measurement in Tecan Infinite M200 plate reader (Tecan Deutschland GmbH, Crailsheim) with the help of Magellan data analysis software (Tecan Austria GmbH, Grödig, Austria).

Assay buffer

110 mM	HEPES
22.2 mM	$MgCl_2$
4.4 mM	ATP
1.8 mM	NAD^+
~0.2 U/reaction	Glucose 6-phosphate dehydrogenase (*Leuconostoc*)

Enzyme dilution

~7 U/reaction	Hexokinase
~0.2 U/reaction	Phosphoglucoisomerase (PGI)
~120 U/reaction	Invertase

In Tecan, 10 cycles were run to determine the basic absorption of the solution at 340 nm. Then 1.3 µl hexokinase, 1.3 µl PGI and 2 µl invertase were added, successively using an enzyme stamp fitting 96 well plates. Each enzyme is added when the end point of the previous step has been reached, i.e. no further increase in absorption can be detected. Calculation of the sugars (glucose, fructose and sucrose) concentration was done applying the original formula of
$\Delta C = \Delta E \times \pi \times r^2 / \varepsilon_{340}$ (NADH) x $V_{M.}$

ΔC = concentration difference
ΔE = change in extinction
r = radius of microtiter plate well
ε_{340} (NADH) extinction coefficient of NADH at 340 nm ($cm^2 \cdot \mu mol^{-1}$)
V_M = volume of assay solution (µl)

For starch measurement, the pellet after ethanolic extraction of soluble sugars was used removing the ethanolic supernatant as complete as possible. The starch pellet was incubated in 900 µl of 0.2 M KOH at 95°C for 1 h. Afterwards, the pH was adjusted to 5.5-6 using approx. 180 µl of acetic acid and the neutralized solution was digested over night at 37°C by adding the 11 µl of an enzyme mixture of ~6 U/reaction amyloglucosidase and ~7 U/reaction α-amylase. The next day, after 5 min centrifugation at 14,000 rpm, 10 µl of the supernatant was used for measurement

with the same assay buffer and the same way as sugars measurement with the exception of adding only 1.3 µl of hexokinase through the measurement.
Extraction and measurement of water-soluble heteroglycans (SHG) were carried out as described in Fettke et al. (2004) in which the unit "nC*min" is a HPAEC-PAD peak area of different monomers. The experiment was performed by Irina Malinova and Jörg Fettke at University of Potsdam, Germany.

2.5 Biochemical methods

2.5.1 Plant protein

2.5.1.1 Protein extraction

Approximately 100 mg frozen leaf material were homogenized to a fine powder in liquid nitrogen, extracted in 100 µl of extraction buffer and incubated on ice for 5-10 min. After centrifugation for 5 min at 14,000 rpm, the supernatant was transferred to a fresh tube and used for enzyme assays and determination of the protein concentration.

Extraction buffer

100 mM	Hepes-NaOH, pH 7.4
1 mM	EDTA, pH 8.0
5 mM	ß-Mercaptoethanol (Carl Roth GmbH & Co KG, Karlsruhe)
50 µg/ml	PMSF in 100% EtOH (AppliChem GmbH, Darmstadt, Germany)

2.5.1.2 Determination of the protein concentration (Bradford assay)

Protein concentration measured using the Bradford assay. 10 µl of the total protein extract were mixed with 990 µl of Bradford assay buffer. The absorption at a wavelength of 595 nm was measured after 10 min of incubation at room temperature in DR 5,000 UV/VIS Spectrophotometer (Hach-Lange). Protein concentration was

quantified using a standard curve prepared from BSA protein (Bovine Serum Albumin) in different known initial concentration of 0, 0.1, 0.2, 0.4, 0.6, 0.8 and 1 mg/ml to reach the 1:100 final concentrations.

Bradford assay buffer

200 µl	Roti-Quant (Carl Roth GmbH & Co KG, Karlsruhe)
800 µl	H_2O

2.5.1.3 PGI activity assay

PGI enzyme activity was measured in a Tecan plate reader. 190 µl of assay buffer per sample was added to each well and absorption was measured at 366 nm. Then, 10 µl of protein extract (10 µg total protein per well and reaction) was measured at 366 nm. The PGI activity was calculated from the slope of NADH production, normalized to the total protein concentration (10 µg/200 µl).

Assay buffer

50 mM	Hepes-NaOH, pH 7.4
1 mM	EDTA, pH 8
3 mM	$MgCl_2$ (Fluka Chemie GmbH, Steinheim, Germany)
3 mM	Fructose 6-phophate-disodium salt hydrate (Sigma-Aldrich Chemie GmbH, Steinheim, Germany)
1 mM	NAD^+
2 µl	in 5 ml assay buffer Glucose 6-phosphate dehydrogenase (from *Leuconostoc mesenteroides,* Roche Applied Science, Mannheim, Germany)

2.6 Pulse amplitude modulated (PAM) fluorometry

Any photosynthetic parameters modifications can be determined *in vivo* by a pulse amplitude modulation (PAM) fluorometer of the IMAGING-PAM Maxi (Heinz Walz GmbH, Effeltrich, Germany) through the changes of chlorophyll a fluorescence.

Ahead of measurement, 3-week-old plants were first incubated in darkness for 30 min. Different variables from a dark-light induction curve were recorded using the default setting of the software i.e., actinic light 8 (186 µmol quanta m^{-2} s^{-1}), slow induction parameters: delay 40 seconds, clock 20 seconds and duration-time 315 seconds. The primary parameters such as the basic (F_0) and the maximal fluorescence (F_m) of dark adapted plants, the variable fluorescence (F_v) the current fluorescence yield (F_t) and the maximal fluorescence after light induction ($F_{m'}$) were determined for the calculation of the maximal quantum efficiency of photosystem II (F_v/F_m), photosynthetic (q_P) and non-photosynthetic (q_N) quench coefficients (Schreiber et al., 1986) and finally, the ETR from light adapted plants (Maxwell and Johnson 2000).

2.7 Staining methods

2.7.1 Starch staining

For starch staining intact leaves/rosettes were incubated in 70% ethanol (v/v) at 60°C until the chlorophyll was removed and the leaves/rosettes had turned white. Subsequently, leaves were stained in iodine-potassium iodide solution (Lugol's solution, AppliChem) for 10 min. Then, the stained materials were washed 3 times over a period of several hours with $H2O_{dd}$ and finally photographed.

2.7.2 Alexander staining

Alexander staining is an indicator of the viability of pollen grains and first introduced by Alexander (1969). Whole filaments were mounted on microscopic glass slides in Alexander staining solution and incubated for 10 minutes. Viable pollen grains display red/purple color since they accumulate the dye, whereas, non-viable pollen grains turned bluish. Images were taken under the light microscope (Eclipse E800; Nikon, Düsseldorf, Germany) using a 1-CCD color video camera (KY-F1030; JVC, Singapore) along with the DISKUS software package (Technisches Buero Hilgers, Koenigswinter, Germany).

Alexander staining solution

10 ml	95% Ethanol
1 ml	Malachite green (1% solution in 95% ethanol)
50 ml	H_2O_{dd}
25 ml	Glycerol
5 ml	Acid fuchsin (1% in H_2O_{dd})
0.5 ml	Orange G (1% in H_2O_{dd})
4 ml	Glacial acetic acid

Add H_2O_{dd} (4.5 ml) to the total volume of 100 ml

2.7.3 DAPI (4', 6-diamidino-2-phenylindole) staining

DAPI staining was used as a measure of goodness for pollen grain physiology and development (Park et al., 1998). Anthers were dissected from the largest unopened flower bud which should contain mature pollen at the tricellular stage. The tricellular stage occurs after pollen mitosis II and consists of a single generative cell and a pair of sperm cells. The dissected anthers were placed on a microscopic glass slide with a droplet of pollen isolation buffer (PIB) containing 3 µg/µl DAPI. Images were taken with a light microscope equipped with the UV fluorescence filter and a 1-CCD color video camera connected to the DISKUS software package.

PIB

100 mM	$NaPO_4$, pH 7.5
1 mM	EDTA
0.1% (v/v)	Triton X-100

2.8 Pollen germination condition

In vitro cultivation of pollen grains was applied for determination of both pollen germination efficiency and pollen tube length. The method was based on Egli et al. (2010) and the Zhengbio Yang laboratory (University of California, Riverside) with some modification. Eight to ten newly opened (0 day) flowers were dissected from plants and incubated at 28°C for 30 min in an empty pipette tip box equipped with

humid filter paper. The pre-hydration helps pollen to germinate at a potentially higher rate (Boavida and McCormick, 2007). Subsequently, flowers were brushed on solid pollen germination medium solidified on a microscopic glass slide and flowers were placed around the brushed pollens because it is known that the flower stigma emits chemical stimulants needed for pollen germination. Alternatively, a droplet of smashed stigma can be added on the medium to induce pollen germination. The slides were then incubated at 37°C for 30 min and afterwards, for 16 h at 28 °C in the dark. Images were taken with a bright field microscope in the same way as previously mentioned (see 2.7.3). Many images as possible were recorded at random positions and the pollen tube length was measured using the ImageJ software.

Pollen germination medium

1 mM	$CaCl_2$
1 mM	$Ca(NO_3)_2$
1 mM	$MgSO_4$
0.01%	H_3BO_3
18%	Sucrose
1.5%	Phyto-Agar (Difco)

2.9 Localization studies

2.9.1 Agrobacterium infiltration of tobacco (*Nicotiana benthamiana*) leaves

Tobacco plants need to be approximately 2 months old to be suitable for infiltration. *Agrobacterium tumefaciens* strain GV3101 containing the vector construct of interest together with the anti-silencing strain RK19 were grown separately at 28°C in YEB medium containing appropriate antibiotics (see 2.11). After one day of incubation, both cultures were centrifuged at 4,000 rpm for 15 min at 4°C. Afterwards, the pellets were resuspended in 1-2 ml of 1x Agro mix and OD_{600} was adjusted to 0.7-0.8. Then, the final filtration solution was prepared by mixing the RK19 and our construct of interest in a ratio of 1:1. The latter mixture was incubated at room temperature for

2-6 h. Finally, the solution was infiltrated to the abaxial part of a leaf using the needleless syringe.

Agro mix solution 10X (100 ml)

2.46 g	100 mM $MgCl_2$.H2O
1.95 g	100 mM MES
Adjusted to pH=5.6	
3 mg/ml in 100% ethanol	Acetosyringon

Agro mix solution 1X (10 ml)

10X 900 µl	Agro mix solution
100 µl	Acetosyringon
9 ml	H_2O_{dd}

2.9.2 Confocal microscopy

Four days after tobacco leaf infiltration, subcellular localization of PGI, cPGI and an empty vector control in leaf cells was analyzed in leaf epidermal cell by spinning-disk confocal microscopy (QLC100 confocal scanning unit from Solamere Technology Group, Salt Lake City, UT attached to a NIKON Eclipse TE 2,000-U bright field microscope) using an argon laser (500M Select, Laserphysics Inc., West Jordan, UT, excitation wavelength filter at 514 nm and emission filter 500-550nm). Images were captured by a CCD-camera (CoolSnap-HQ, Photometrics, Tucson, AZ) using the Metamorph software (Universal Imaging Corporation, Downington, PA).

2.10 Transformation

2.10.1 Transformation of *Arabidopsis thaliana*

For plant transformation, the floral dip method (Clough and Bent, 1998) was used. For this approach, 50 ml of YEB medium supplemented with the appropriate selection marker (see 2.11) were inoculated with the Agrobacterium strain of interest

and pre-cultured at 28°C and 220 rpm on a shaker over night. The preculture was diluted into 300 ml of pre-warmed YEB medium and incubated for one more day. When the main culture had reached an OD_{600} of 0.8, it was centrifuged at 4,000 rpm for 15 min at 4°C. The cell pellets were added to the transformation solution and plant inflorescences were dipped into the solution for 10 seconds. Freshly transformed plants were laid sideways in the tray and covered with a water-sprayed plastic lid maintained high humidity conditions. Trays were then placed in dim light conditions. After a day, plants were stood up in trays and transferred to the greenhouse. The positive T1 individuals were selected on kanamycin and hygromycin resistance plates conferred by pGWB2.

Transformation solution

5%	Sucrose
0.05%	Silwet ® Gold (Spiess-Urania)

Adjusted with H_2O_{dd} to a total volume of 50 ml

2.10.2 Transformation of *E. coli* bacteria

Transformation of *E. coli* bacteria was carried out applying the heat-shock method. One microliter of plasmid DNA was added to 50 µl of *E. coli* competent cells while cells were thawing on ice. Then the cells were placed in water bath at 42°C for 90 seconds. Immediately after the heat shock, 1 ml of LB medium was added to the cells and diluted cells were allowed to recover at 37°C for 1 h in an orbital shaker (220 rpm). After 1 h of incubation, the cells were pelleted and resuspended in a small volume of LB and spread out on selective LB plates.

2.10.3 Transformation of *Agrobacterium tumefaciens*

The chemical heat-shock method was used for transformation of agrobacteria using 2 µl of the plasmid of interest. The tube was gently shaken by hand and placed in liquid nitrogen. After a few seconds, the tube was heated to 42°C in a water bath for 90 seconds. Subsequently, 1 ml YEB medium was added to the tube. After

incubation of 2 h at 28°C in an orbital shaker and centrifugation for 1 min, the pellet was evenly spread on YEB plate with the proper antibiotics according to both agrobacteria strain and expression vector (see 2.11). Plates were incubated at 28°C in oven for about 2 days.

2.11 Selection markers

2.11.1 Vector selection markers

Vector name	**Selection markers**
pGWB2	Kan. (50 µg/µl), Hyg. (50 µg/µl)
pAMPAT	Carb. (100), BASTA
pHygII-UT-c-term-Venus	Kan. (50 µg/µl), Hyg. (50 µg/µl)
pENTR D-TOPO	Kan. (50 µg/µl)

Antibiotics	**Stock solution**	**Dissolved**
Kanamycin (Kan.)	50 mg/ml	in $H2O_{dd}$
Hygromycin (Hyg.)	50 mg/ml	in $H2O_{dd}$
Carbincillin (Carb.)	50 mg/ml	in $H2O_{dd}$

2.11.2 Agrobacterium selection markers

Agrobacterium strains	**Antibiotic selection markers**
GV3101	Gent. (25 µg/ml), Rif. (150 µg/ml)
GV3101 (pMP90RK).	Kan. (25 µg/ml), Rif. (50 µg/ml)
RK19	Kan. (50 µg/ml), Rif. (150 µg/ml)

Antibiotics	**Stock solution**	**Dissolved**
Kanamycin (Kan.)	50 mg/ml	in H_2O_{dd}
Gentamycin (Gent.)	25 mg/ml	in H_2O_{dd}
Rifamycin (Rif.)	30 mg/ml	in DMSO

2.11.3 Plant selection markers

2.11.3.1 Antibiotic selection

Antibiotic/antibiotics were added as appropriate to autoclaved ½ MS medium after cooling down to the hand warm level. Selection of transformed plants was performed on hygromycin and/or kanamycin (50 µg/ml each) containing plates.

Antibiotics	**Stock solution**	**Dissolved**
Kanamycin (Kan.)	50 mg/ml	in H_2O_{dd}
Hygromycin (Hyg.)	50 mg/ml	in H_2O_{dd}

2.11.3.2 BASTA selection

Plants harboring the resistance gene for the herbicide BASTA/glufosinate, were sprayed with BASTA solution (1%, v/v) after cotyledons appeared. Spraying was repeated after 2 days.

1% BASTA solution

250 mg/l	BASTA ®
0.1%	Tween-20

2.12 Primers

Primers used for PCR amplification

Primer pairs name	Primer pairs sequence
ActinI fwd	TGCGACAATGGAACTGGAATG
ActinI rev	GGATAGCATGTGGAAGTGCATAC
LBaI left border SALK primer	TGGTTCACGTAGTGGGCCATCG
GABI left border	CCCATTTGGACGTGAATGT
cPGI fwd5	GAGTCTGCTAAAGGACGCCAG
cPGI rev10	GCAAGATTAGTGCTGACAGCAAC
cPGI fwd7	TCTGTGTTTCTGTTCGCAATG
cPGI rev12	TGGGTGAGAAATGAATCCAAC
cPGI fwd2	AATTGCAACGAATTTCACTCG
cPGI rev9.5	CTCAATGTTCTGGCGTTAAGC
cPGI s	BamHI GGATCCAAAATGGCGTCATCAACCGC
cPGI as	XmaI CCCGGGCATCTGGGGCTCGGAAC
PGI s	XbaI TCTAGAAAATGGCCTCTCTCTCAGGCC
PGI as	XmaI CCCGGGTGCGTACAGGTCATCCACATT
FUM2 fwd3	GGGAAGCCATAATGGAAG
FUM2 rev5	GTCAAAGGTGTAGCATCTTGAG
I miR1-s	GATGTACTGTTAATATGCTCCCGTCTCTCTTTTGTATTCC
II miR1-a	GACGGGAGCATATTAACAGTACATCAAAGAGAATCAATGA
III miR1*s	GACGAGAGCATATTATCAGTACTTCACAGGTCGTGATATG
IV miR1*a	GAAGTACTGATAATATGCTCTCGTCTACATATATATTCCT
I miR2-s	GATATCTAGAACGTTCCAGACTTTCTCTCTTTTGTATTCC
II miR2-a	GAAAGTCTGGAACGTTCTAGATATCAAAGAGAATCAATGA
III miR2*s	GAAAATCTGGAACGTACTAGATTTCACAGGTCGTGATATG
IV miR2*a	GAAATCTAGTACGTTCCAGATTTTCTACATATATATTCCT

3. Results

3.1 Tissue specific expression of PGI isoenzymes

According to publicly available expression data, both PGI isoenzymes are highly expressed in leaf tissues at approximately the same level (Winter et al., 2007; eFP-Browser; http://bar.utoronto.ca/efp/cgi-bin/efpWeb.cgi). However, in other tissues transcript abundance of cPGI is higher during embryonic stages and seed development while transcript of the plastidic isoform is more abundant in the root, particularly in columella and vascular tissue. In root, the *cPGI* expression is more in the meristematic, elongation and maturation zones.

3.2 Subcellular localization of plastidic and cytosolic PGI

According to activity gel assays (Caspar et al., 1985; Yu et al., 2000) and *in silico* analysis (Schwacke et al., 2003), PGI1 localizes to the chloroplast while Arabidopsis proteome analysis (Ito et al., 2011) indicated that cPGI localizes to the cytosol. To confirm the predicted subcellular localization of both PGIs *in vivo*, PGI and cPGI reporter gene fusion proteins were generated employing the plant destination vector pUBQ10:pHygII-UT-c-term-Venus. This vector enables expression of the yellow fluorescent protein (YFP) Venus driven by the ubiquitin-
10 promoter as a C-terminal fusion to the full-length coding sequence of PGIs. The construct was transiently expressed in *N. benthamiana* leaves together with the anti-silencing strain RK19.
Confocal microscopy demonstrates the plastidic localization of the PGI1::Venus fusion protein since chlorophyll autofluorescence and the YFP signal co-localized in *N. benthamiana* leaf cells transiently expressing the fusion protein (Figure 3A). In contrast the cPGI::Venus fusion protein does not co-localize with chlorophyll autofluorescence, indicating a cytosolic localization (Figure 3B). Figure 3C depicts a strong YFP signal from both cytosol and nucleus for the empty vector control which is clearly different from a solely cytosolic localization as observed for the cPGI::Venus protein.

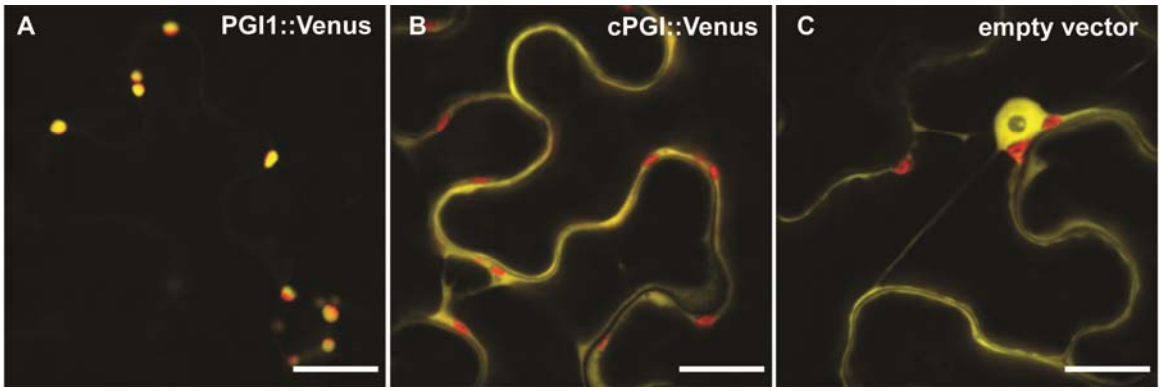

Figure 3: Subcellular localization of PGI1 and cPGI. (A) PGI1 and (B) cPGI Venus fusion proteins (yellow) are localized to chloroplasts (red) and the cytosol, respectively. (C) An unfused Venus protein expressed from the empty vector was used as control. Constructs were transiently expressed in *Nicotiana benthamiana* leaves. All images are merged with the corresponding chlorophyll autofluorescence image (red). Scale bar = 20 µm.

3.3 Identification of T-DNA target sites for *cPGI*

Two independent T-DNA lines (Alonso et al., 2003) with insertions in the *cPGI* coding region were obtained from the Nottingham Arabidopsis Stock Center (NASC). The T-DNAs are inserted in the ninth exon and in the seventh intron in lines *cpgi-1* and *cpgi-2*, respectively (Figure 4A). Genotyping of more than 300 plants from the progeny of heterozygous mother plant identified only heterozygous and wild-type plants but no homozygous individuals (Figure 4B). The ratio of heterozygous to the total number of genotyped plants was 148/ 304 for *cpgi-1* and 159/305 for *cpgi-2*. The results suggest a ratio of 1:1:0 for wild-type, heterozygous and homozygous mutants which indicate that homozygous mutants may be lethal.

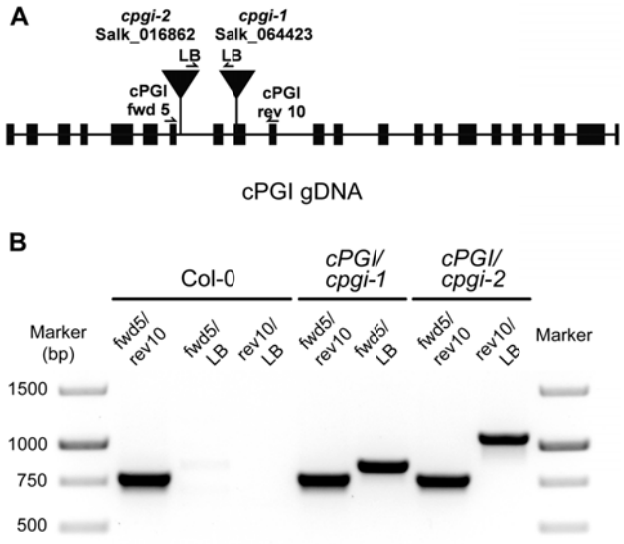

Figure 4: Identification of T-DNA insertion sites in the *cPGI* coding region. (A) Two independent *cPGI* insertion lines (*cpgi-1*, *cpgi-2*) were isolated and the insertion site confirmed at the positions indicated. (B) Confirmation of T-DNA insertions in *cPGI/cpgi-1 and cPGI/cpgi-2* by genomic DNA PCR using primers indicated in A. No homozygous plants could be identified.

3.4 Generation of artificial microRNA (amiR) *cpgi* mutants

An alternative to analyzing T-DNA loss-of-function lines is the characterization of lines expressing artificial micro RNAs (amiRNAs) designed against the gene of interest. Often this sort of mutants represents knock-down rather than knock-out mutants. Therefore, two different amiRNAs targeting different regions of the *cPGI* mRNA were designed and transformed into Col-0 wild-type plants (Figure 5). For both amiRNAs several independent lines were isolated and analyzed. All experiments were performed using two independent lines for amiRNA1 named amiR-*cpgi 6* and amiR-*cpgi* 10. However, to reconfirm the phenotypes related to amiRNA1 lines, key experiments were repeated on three independent lines of amiRNA2 labeled amiR2-*cpgi 8*, *9* and *10*.

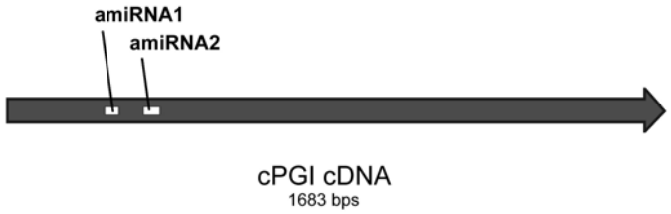

Figure 5: Position of target sites of two independent artificial micro RNAs (amiR) designed against *cPGI* mRNA.

3.5 Total and cytosolic PGI activity of amiRNA1

To assess the impact of amiRNA expression on total and cytosolic PGI activity, enzyme assays with total protein extracts from leaves of ten different amiRNA1-*cpgi* lines were performed and compared to extracts from *pgi1-1* and Col-0 as controls. Results show a strong reduction of total PGI activity for all ten mutant lines to less than 40% of wild-type activity and for *pgi1-1* to about 80% of wild-type (Figure 6A). The cytosolic activity can be determined by getting rid of the plastidic activity through heating of the protein extract to 50°C for 10 min before performing the enzyme activity assay (Jones et al., 1986b; Yu et al., 2000). Pre-heated protein extracts revealed a cytosolic PGI activity in amiR-lines of less than 1% of the wild-type (Figure 6B). The left-over total PGI activity of these plants might be either attributed to plastidic PGI not fully inactivated during heat treatment or residual cytosolic PGI activity due to incomplete knock-down of *cPGI* mRNA. According to these results, amiR-*cpgi 6* and *10* showed an activity of cytosolic PGI close to zero and were selected for further analyses.

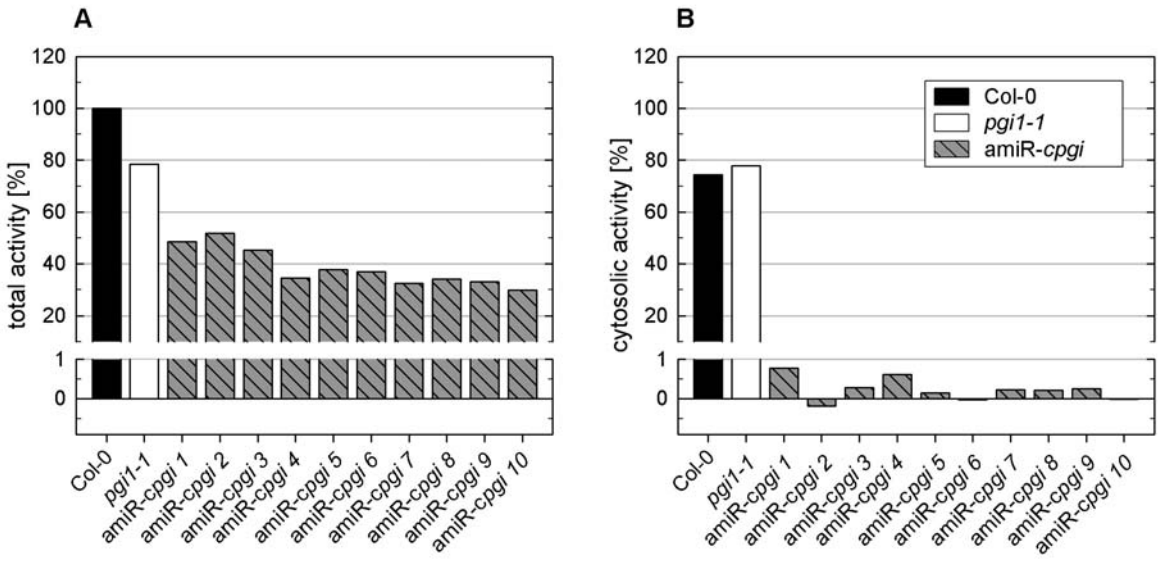

Figure 6: Reduced PGI activity in amiRNA1-*cpgi* plants. (A) Total PGI activity and (B) cytosolic PGI activity after heat inactivation of plastidic PGI in leaf extracts of ten independent amiR-*cpgi* lines. Rates were normalized to total activity in leaf extracts from Col-0 wild-type (100% corresponds to an activity of 0.219 nmol • (µg total protein • min)$^{-1}$).

3.6 Growth phenotype, leaf area and rosette fresh weight of amiRNA1-*cpgi*

Comparing three-week-old amiRNA1-*cpgi* lines *6* and *10* with Col-0 revealed no growth abnormalities in color or in shape. However, a reduced vegetative growth of amiR-lines compared to the wild-type could clearly be observed (Figure 7A). In particular, the growth phenotype was more pronounced for the amiR-*cpgi* plants and starch-free mutant *pgi1-1* in short-day conditions compared to long-day conditions (Figure 8A, B). Quantification of growth by measuring leaf area and rosette fresh weight of amiR-*cpgi*, *pgi1-1* and Col-0 revealed significantly smaller leaf area and lower rosette fresh weight of all mutants compared to the wild-type (Figure 7B). Reduced vegetative growth has been reported previously for *pgi1-1* and other mutants impaired in carbohydrate metabolism such as *pgm* (Gibon et al., 2009; Izumi et al., 2013). To be able to better evaluate the growth reduction phenotype of amiR-*cpgi* plants, mutants impaired in other cytosolic pathways with impact on plastidic carbohydrate metabolism such as *dpe 2-1* and *dpe 2-2,* defective in heterogylcan turnover (Lu and Sharkey, 2004) or *fum 2*, reportedly over accumulating starch in chloroplasts (Pracharoenwattana et al., 2010) were analyzed for comparison (Figure 8A, B). Similar to other mutants defective in carbohydrate metabolism, *dpe2* mutants displayed a reduced growth phenotype in long-day and short-day conditions (Figure 8A, B). In contrast, *fum2* mutant lines produced more biomass and rosette leaf area compared to wild-type (Figure 8A, B).

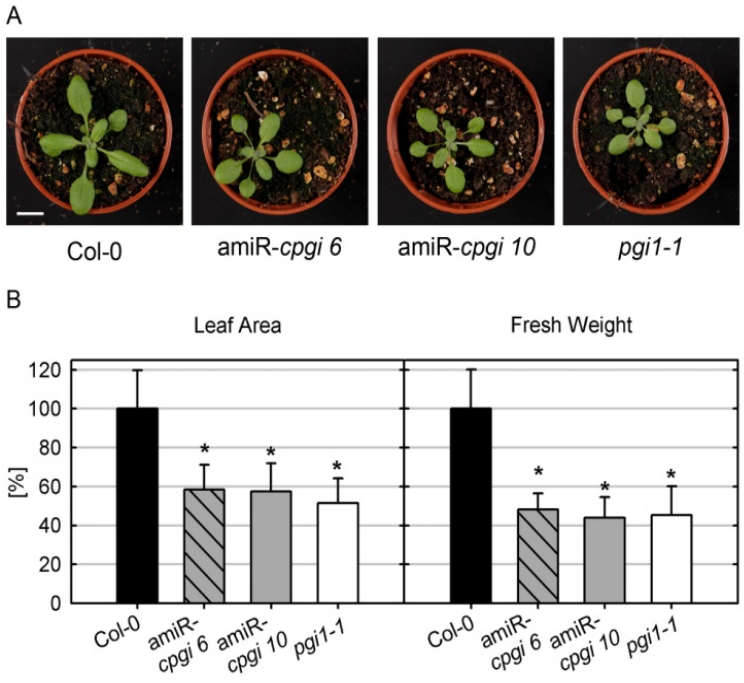

Figure 7: Growth phenotype of amiRNA1-*cpgi* lines and *pgi1-1* mutants. (A) Col-0, amiR-*cpgi 6*, amiR-*cpgi 10* and *pgi1-1* grown on soil in long-day conditions for 21 days. Scale bar = 1 cm. (B) Relative leaf area and rosette leaf fresh weight of wild-type and mutant plants grown on soil in long-day conditions for 21 days. Bars represent averages ± SD from 3 independent experiments (n = 15-30). Asterisks indicate significant difference to wild-type (student's t-test, a ≤ 0.01).

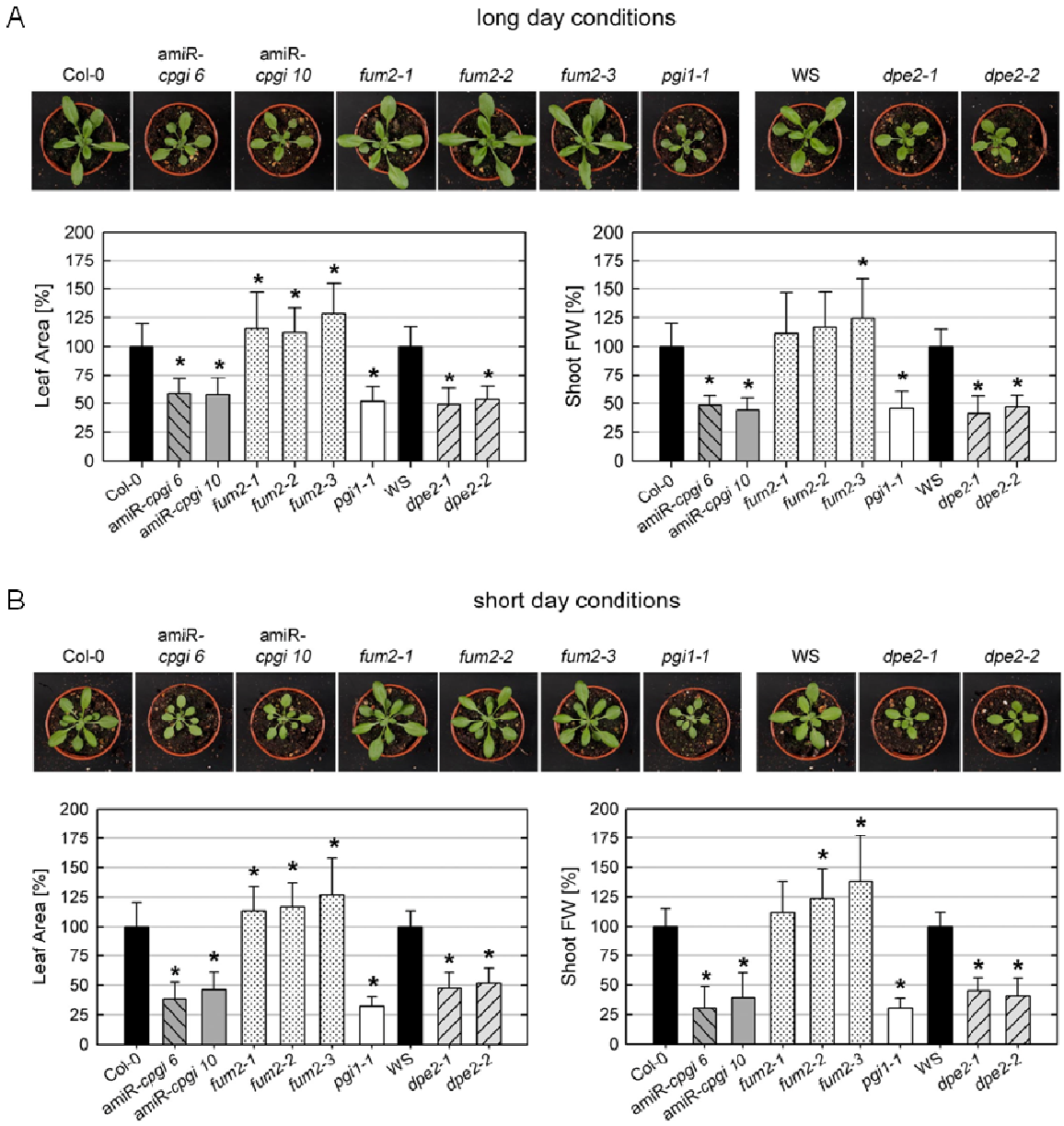

Figure 8: Plant growth of mutants and corresponding wild types in long- and short-day conditions. (A) Leaf area and shoot fresh weight of different plant lines normalized to wild-type after growth for 21 days in long-day conditions. (B) Leaf area and shoot fresh weight of different plant lines normalized to wild-type after growth for 21 days in short-day conditions. Data represent averages ± SD from 3 independent experiments (n = 15-30). Asterisks indicate significant differences to wild-type (student's t-test, $\alpha \leq 0.05$). Wassilewskija (WS) accession is the corresponding wild-type for *dpe2* mutants. All other mutants are in Columbia-0 (Col-0) background. Due to general growth variation between replicate experiments data were normalized relative to wild-type [%].

3.7 PAM measurement indicates increased non-photochemical quenching and reduced photosynthetic electron transport in amiR-*cpgi* mutants

3.7.1 amiRNA1-*cpgi* mutant lines

PAM fluorometry can be used as an indicator for intactness of photosystems in chloroplasts and photosynthetic activity in general. Since amiRNA1-*cpgi* mutants revealed a reduced growth phenotype, PAM analysis was applied to investigate whether photosynthesis was affected in these mutants. The ratio of variable over maximal chlorophyll fluorescence (Fv/Fm) is being used for determination of the maximum quantum efficiency of photosystem II. The Fv/Fm ratio of 0.8 in leaves of 30 min dark-adapted mutant and wild-type plants indicated an intact photosystem II with no differences between mutants and wild-type (Figure 9A). On the other hand, the non-photochemical quench coefficient (q_N) was higher in amiRNA1-*cpgi* mutants compared to wild-type. In whole plant, false-color imaging PAM pictures areas of higher non-photochemical quenching appear in dark blue colors (Figure 9B). In addition to increased non-photochemical quenching in amiR1-*cpgi* plants, photosynthetic induction curves also revealed decreased photochemical quench coefficient (q_P) along with decreased electron transport rates (ETR) in amiR1-*cpgi* plants (Figure 9C). This may suggest that alteration of the photosynthetic light reaction within the chloroplast's thylakoids is a specific result of cytosolic PGI deficiency considering that *dpe2-1* and *dpe2-2* showed no or only very minor impact on non-photochemical quenching in compare to its related wild-type (Figure 10). In experiments with amiR1-*cpgi* plants of later generations we noticed that the effect of the amiRNA disappeared. Therefore, we took advantage of the increased NPQ as selection criterion for amiR-*cpgi* mutants instead of using selective antibiotic plates, with the idea of exposing mutant plants to as little stress as possible prior to biochemical analyses.

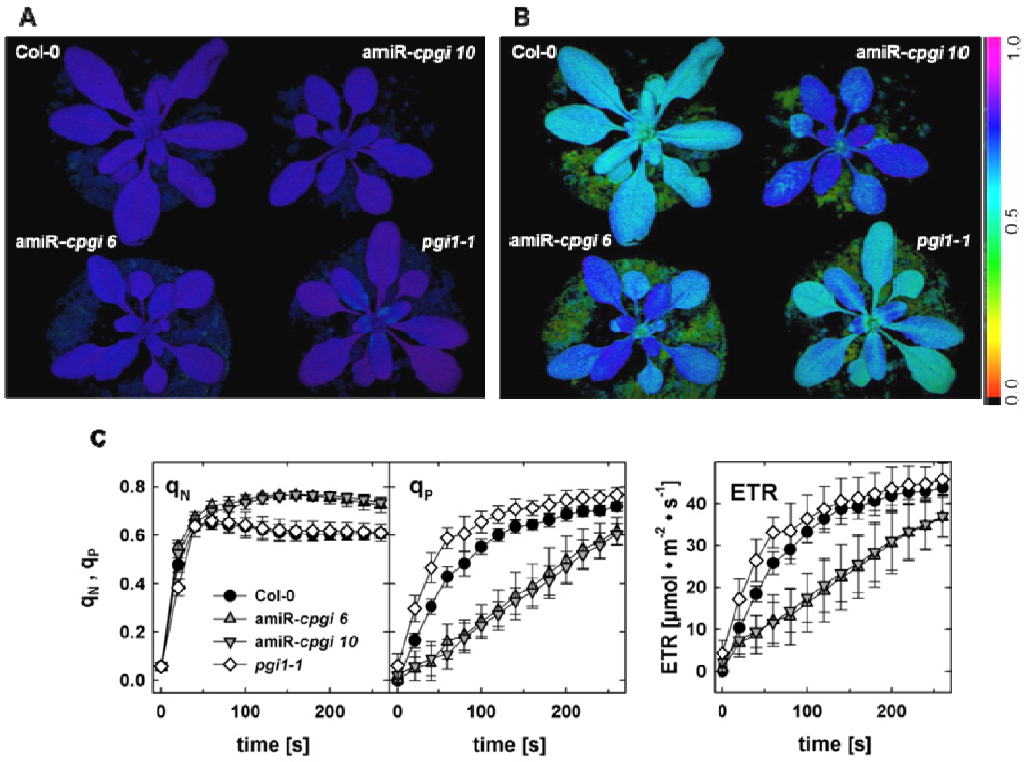

Figure 9: Pulse Amplitude Modulated (PAM) fluorescence imaging. (A) The variable over maximal fluorescence ratio (F_v/F_m). Blue-purple false colors in leaves of all plants indicate an F_v/F_m of about 0.8 which is typical for plants with intact PSII. (B) Non-photochemical quenching (NPQ). (C) Non-photochemical (q_N) and photochemical (q_P) quench coefficients and photosynthetic electron transport rates (ETR) during light induction curves determined by PAM fluorescence imaging in rosette leaves of wild-type, amiRNA1-*cpgi 6* and *10* and *pgi1-1* plants. Average ± SD (n = 15).

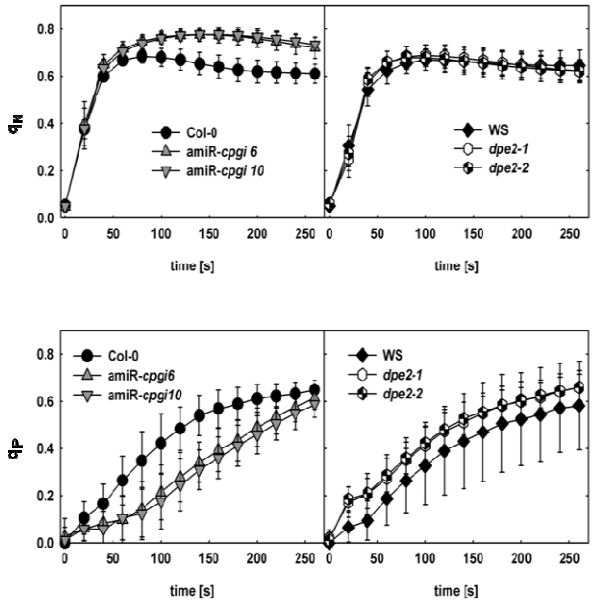

Figure 10: Non-photochemical (q_N) and photochemical (q_P) quench coefficients during light induction curves in amiRNA1-*cpgi* and *dpe2* mutants and corresponding wild-type plants grown in long-day conditions. Average ± SD (n = 36-60).

3.7.2 amiRNA2-*cpgi* mutant lines

Conducting the experiments with second amiRNA lines *8*, *9* and *10* indicated the same results as the first amiRNA-*cpgi* mutant (for comparison see 3.7.1). These results also revealing the increased non-photochemical quench coefficient (q_N) in amiRNA2-*cpgi* lines, as well as the reduced photochemical quench coefficient (q_P) and electron transport rate (ETR) (Figure 11).

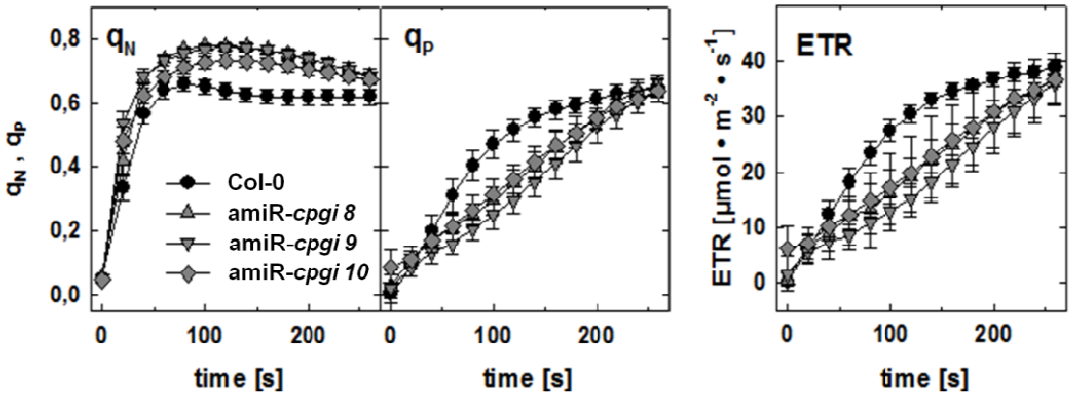

Figure 11: Non-photochemical (q_N) and photochemical (q_P) quench coefficients and photosynthetic electron transport rates (ETR) during light induction curves determined by PAM fluorescence imaging in rosette leaves of wild-type, amiRNA2-*cpgi* lines *8*, *9* and *10* together with Col-0 plant.

3.8 Starch excess phenotype in mature leaves of amiRNA-*cpgi* mutants

3.8.1 amiRNA1-*cpgi* mutant lines

Since cPGI is involved in carbohydrate metabolism, starch staining and starch content measurements were performed. It is generally accepted that transitory starch accumulating during the light period is degraded during the subsequent night period to sustain metabolism, growth and development. Absence of starch in the wild-type at the end of the night is a result of this diurnal cycle. Results of staining with Lugol's solution showed strongly increased starch levels at the end of the night in amiR1-*cpgi* plants (Figure 12A). To further confirm the starch excess phenotype, the starch content was measured at different time points during the day. Results indicated

significantly increased starch content at the end of the night in leaves of amiRNA1-*cpgi* mutants compared to wild-type plants and the almost starch-free mutant *pgi1-1* (Figure 12B).

To investigate any correlation between an increased NPQ (Figure 9B, C) and a starch excess phenotype (Figure 12), starch staining was carried out for two other known starch excess mutants, namely *fum2* (Pracharoenwattana et al., 2010) and *dpe2* mutants (Lu and Sharkey, 2004). Surprisingly, none of the *fum2* mutant lines showed a starch excess phenotype in the current experiment (Figure 13), although the growth condition and time of harvesting were the same for all plant genotypes. However, *dpe2* mutants showed a high starch level as previously reported (Figure 13).

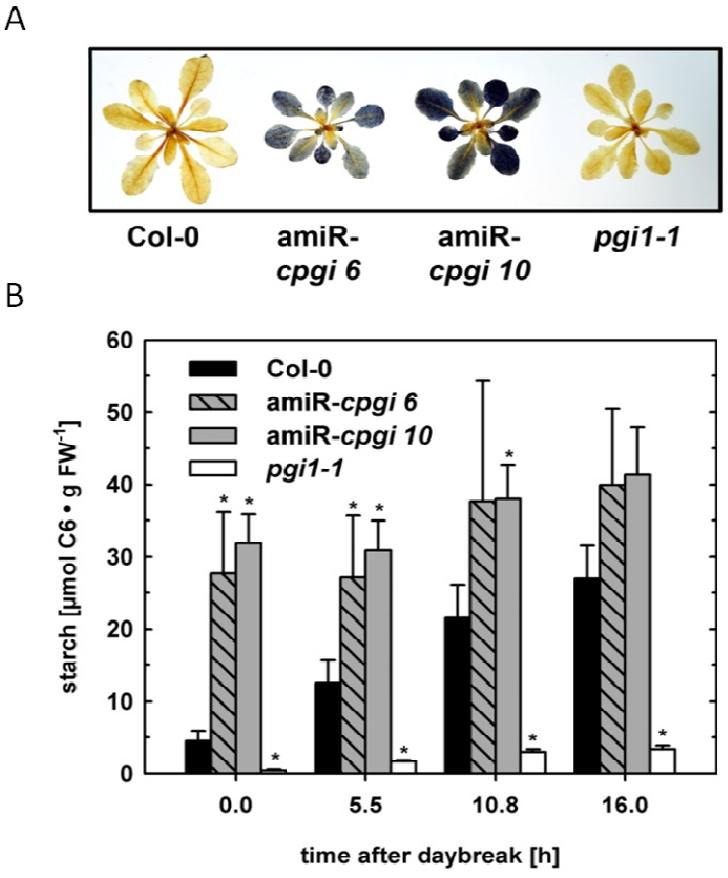

Figure 12: Starch excess in leaves of amiRNA1-*cpgi* plants. (A) Starch staining of whole leaf rosettes harvested at the end of the regular night period. (B) Starch content of wild-type, amiR-*cpgi 6*, amiR-*cpgi 10* and *pgi1-1* leaves at different time points during the light period. Average ± SEM. n=3. Asterisks indicate significant difference to wild-type of the same time point (student's t-test, $\alpha \leq 0.05$).

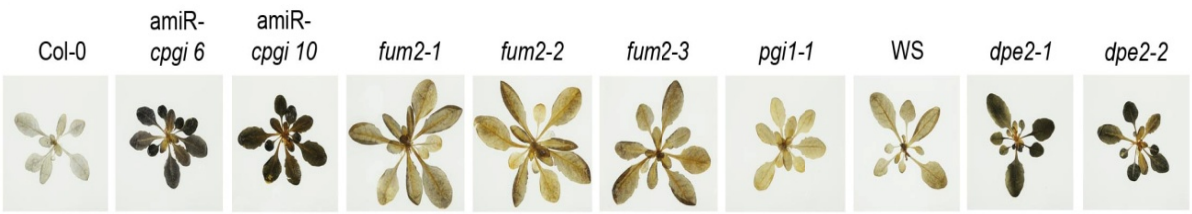

Figure 13: Starch staining of whole rosettes harvested at the end of the night from long-day grown plants.

3.8.2 amiRNA2-*cpgi* mutant lines

In order to indepentenly confirm the starch excess phenotype of amiRNA1 lines at the end of the night, these measurements were repeated for three lines of amiRNA2 at the end of the day and the night (Figure 14A, B). amiRNA2-*cpgi* lines revealed the same phenotypes as the first amiRNA regarding the elevated leaf starch content at the end of the night (Figure 14A, B).

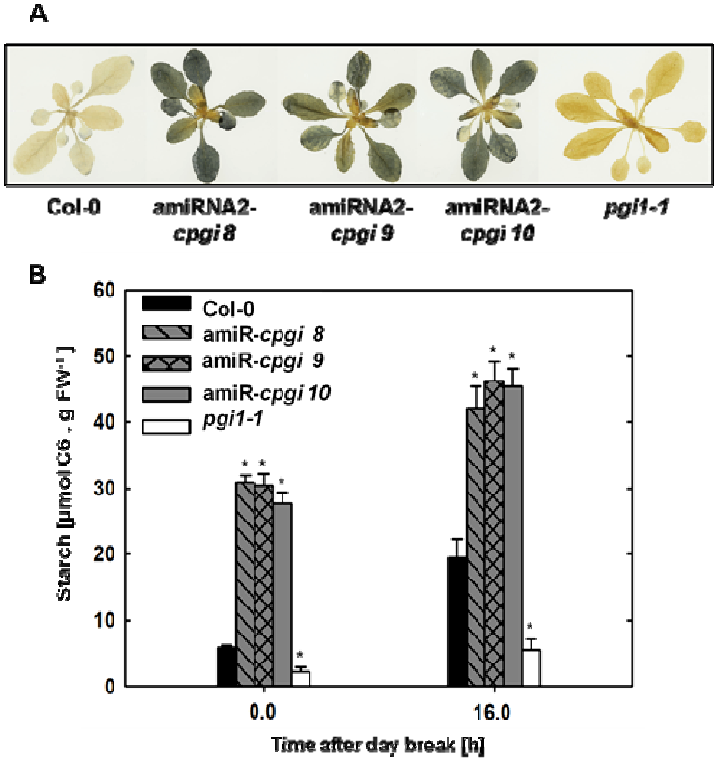

Figure 14: Starch excess in leaves of amiRNA2-*cpgi* plants. (A) Starch staining of whole leaf rosettes harvested at the end of the regular night period. (B) Starch content of wild-type, amiRNA2-*cpgi 8*, *9, 10* and *pgi1-1* leaves at the end of the day and the night. Average ± SEM. Asterisks indicate significant difference to wild-type of the same time point (student's t-test, $\alpha \leq 0.05$).

3.9 Sucrose and cytosolic heteroglycans content in mature leaves of amiRNA-*cpgi* mutants

3.9.1 amiRNA1-*cpgi* mutant lines

Since cPGI is a key enzyme in sucrose synthesis and lack of its activity appeared to feed back on starch turnover (see 3.8), analysis of sucrose content at the same time points as starch measurement was coupled with analysis of the monosaccharide composition of cytosolic heteroglycans at the end of the night. The sucrose content showed a high variability between replicate experiments for time points during the day and no detectable difference between amiR1-*cpgi* mutants and wild-type. However, the leaf sucrose content of amiRNA1-*cpgi* lines was significantly lower compared to wild-type at the end of the night (Figure 15A).

Moreover, determination of the monosaccharide composition of soluble heteroglycans (SHGs), an interim monosaccharide storage molecule for starch degradation products, revealed a significant increase of glucose among SHGs monomers in lines *6* and *10* of amiRNA1-*cpgi* mutants compared to wild-type (Figure 15B). The increase of glucose content in cytosolic SHGs can be explained by excess glucose derived from maltose breakdown that cannot be channeled into the sucrose synthesis pathway due to the lack of cPGI activity. Assaying of SHGs composition was carried out over the range of low (<10 kDa) and high (>10 kDa) SHGs molecular weight. The amount of galactose as a major heteroglycan's monomer is constant between ecotypes and was used for normalization (Figure 15B).

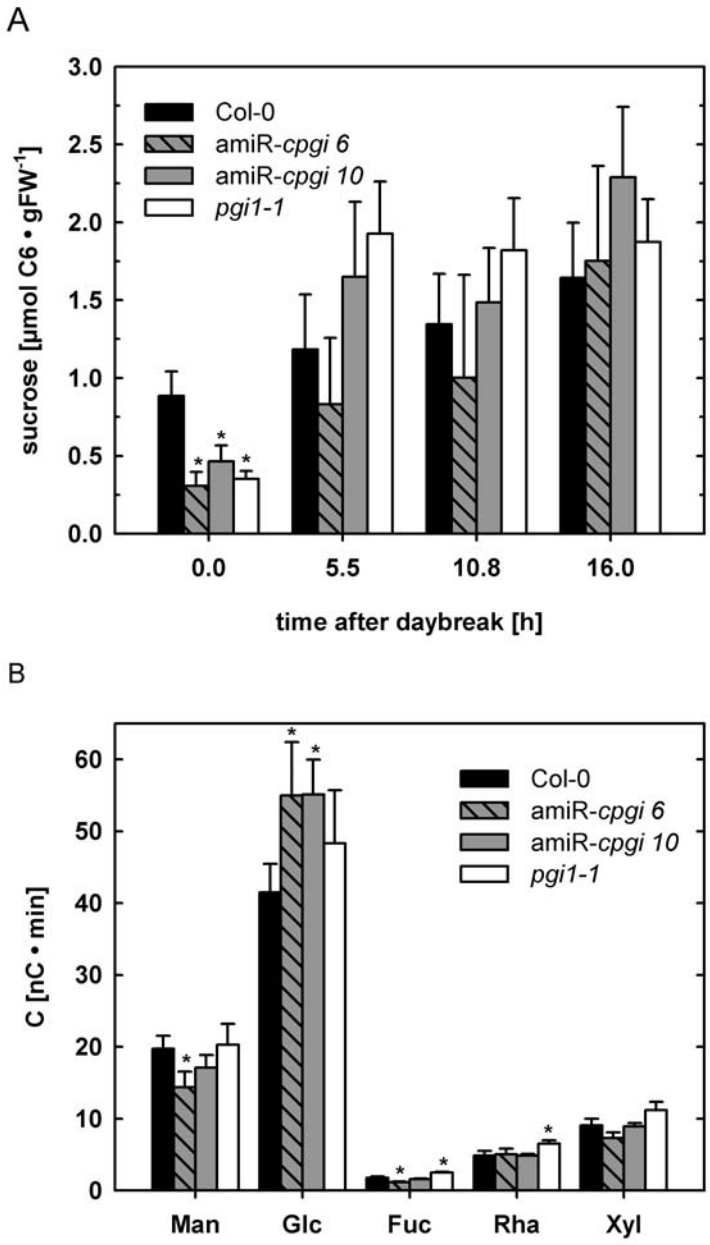

Figure 15: Sucrose content and relative monosaccharide composition of cytosolic heteroglycans in leaves. (A) Sucrose concentration in wild-type, amiRNA1-*cpgi 6*, *10* and *pgi1-1* leaves at different time points during the light period. Average ± SEM. n=3. (B) Monomer composition of low molecular weight (<10 kDa) cytosolic heteroglycans (SHGs) in leaves of wild-type, amiR-*cpgi 6*, amiR-*cpgi 10* and *pgi1-1* plants at the end of the night. Data were normalized to the major heteroglycan-monomer galactose. Average ± SEM. n = 6. Asterisks indicate significant difference to wild-type of the same time point (student's t-test, $\alpha \leq 0.05$).

3.9.2 amiRNA2-*cpgi* mutant lines

The sucrose content measurement was carried out on three lines of amiRNA2-*cpgi* (*8*, *9* and *10*) at the end of the day and the end of the night for confirmation of this phenotype seen before for the first amiRNA lines (see 3.9.1). The results of amiRNA2-*cpgi* mutants were in line with previous results in which sucrose content were low at the end of the night in compare to wild-type (Figure 16).

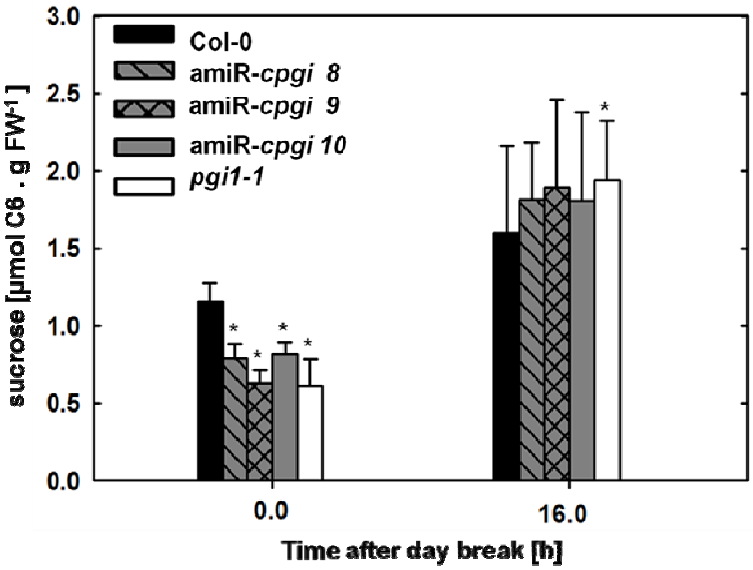

Figure 16: Sucrose concentration in leaves of amiRNA2-*cpgi* plants at the end of the day and the night. Average ± SEM. Asterisks indicate significant difference to wild-type of the same time point (student's t-test, $\alpha \leq 0.05$).

3.10 Determination of transitory starch effects on viability of amiRNA1-*cpgi* mutants

Since impaired cPGI enzyme activity led to starch over accumulation, it was hypothesized that metabolism and vitality of plants simultaneously lacking cPGI activity and the ability to generate transitory starch might be strongly compromised. To investigate this hypothesis, two nominally starch-free mutants defective in either ADP-glucose pyrophosphorylase (*adg1-1*) or plastidic PGI (*pgi1-1*) were transformed

with the *cpgi* amiRNA1. Transformed plants were selected on ½ MS plate supplemented with 2% sucrose and the respective antibiotics.

Selected plants were subsequently transferred to soil. Interestingly, after 21 days, all plants were stunted in growth, displayed very small paled leaves and failed to develop into adult plants and produce seeds (Figure 17A). On the other hand, plants which were maintained on ½ strength MS medium in the presence of 2% sucrose but without antibiotic were considerably bigger and produced rosette leaves in compare to plants grown on soil (Figure 17A). These plants could further develop up to the flowering stage and even produced a few seeds (Figure 17B). These data indicate that feeding exogenous sucrose can alleviate the strong growth retardation phenotype observed in these plants on soil.

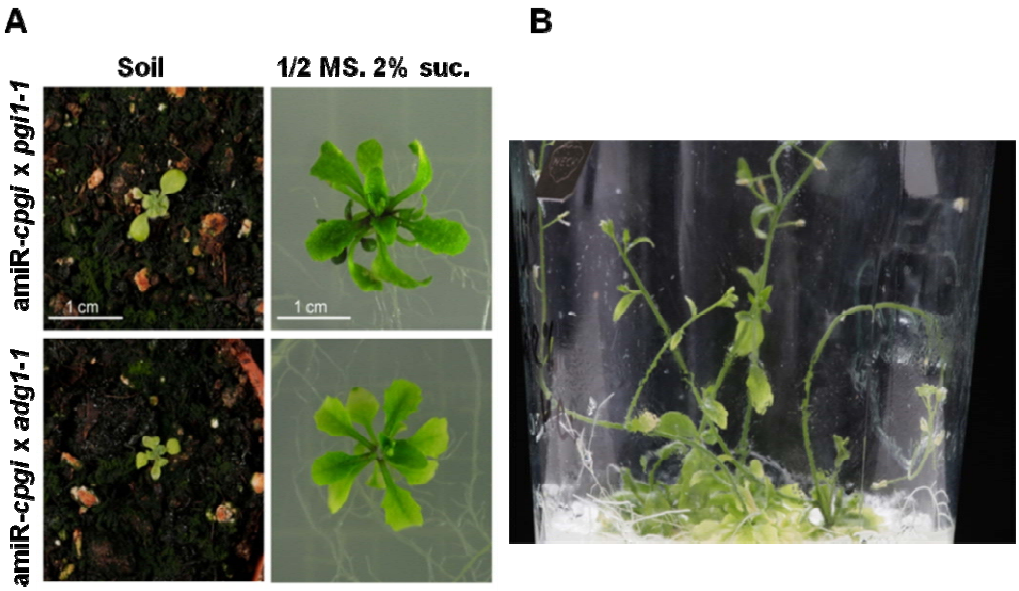

Figure 17: (A) Phenotype of plants expressing *cpgi* amiRNA1 in the virtually starch-free mutant background of *pgi1-1* or *adg1-1* after 21 days of growth on soil or sucrose-supplemented (2%) solidified ½ strength MS medium. (B) *In-vitro* cultivation of amiR-*cpgi* x *adg1-1* in the presence of 2% exogenous sucrose.

3.11 Analysis of male gametophyte through pollen of *cpgi* T-DNA mutants

Although the availability of amiRNA-*cpgi* mutants enabled characterization of reduced cPGI activity on metabolism of adult plants, having no homozygous T-DNA mutant remained an enigma. Absence of homozygous T-DNA insertion mutants can point to fatal defects at different developmental stages. First, one of the gametophytes might essentially require cPGI activity for proper development or vitality. Secondly, failing to isolate homozygous T-DNA mutants in a segregating seed population might also indicate embryo lethality of homozygous mutants.

As a first approach, Alexander staining of mature pollen was used as a measure to determine pollen viability, i.e. male gametophyte vitality, from heterozygous *cPGI/cpgi-1* and *cPGI/cpgi-2* anthers. In Alexander staining, viable pollens accumulate the stain and become red/purple, whereas non viable pollens remain bluish (Figure 18A). However, pollen grains from heterozygous mutants did not stain differently from wild-type pollen indicating that viability of mutant pollen might not be affected (Figure 18A).

DAPI staining is a measure of pollen nuclei intactness staining the DNA in pollen grains. Mature pollen contains three nuclei at the so called tricellular stage, which develops after the second pollen mitosis. These pollen grains contain one vegetative and two generative cells. DAPI staining of mutant pollen grains showed no differences in shape of pollen grains or pollen maturity compared to wild-type (Figure 18B). Finally, the mutant pollen grain germination of both *cPGI/cpgi-1* and *cPGI/cpgi-2* showed a similar pattern as wild-type (Figure 18C). Pollen tube length measurement of approximately 500 germinated pollen grains revealed that pollen tube length of mutant pollen did not significantly differ from wild-type pollen for both heterozygous *cpgi* T-DNA lines (Figure 19).

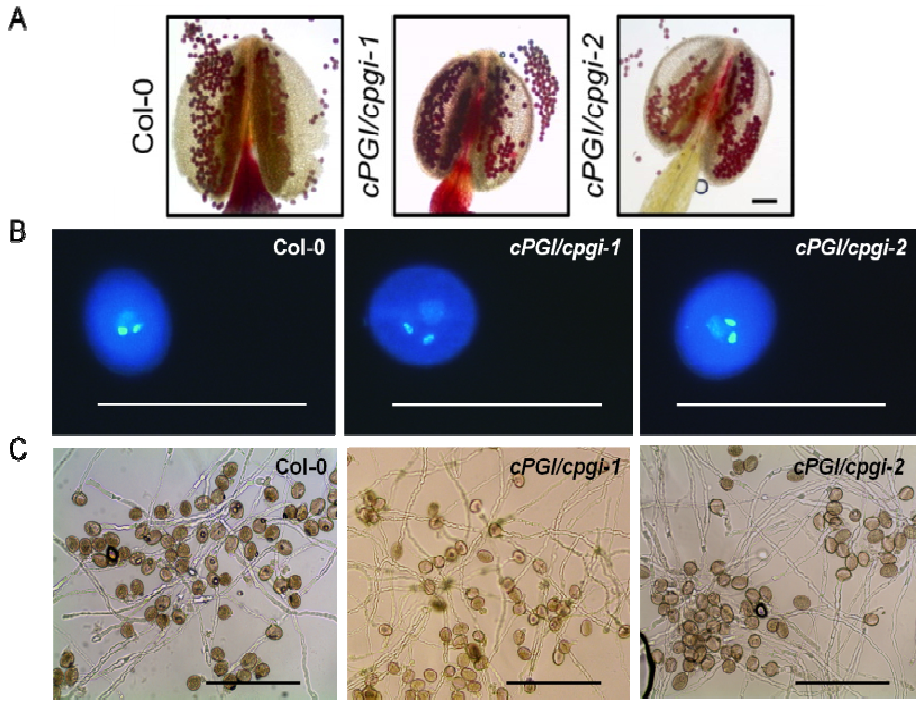

Figure 18: Pollen assessment of *cPGI/cpgi-1* and *cPGI/cpgi-2* in compare to Col-0. (A) Bright field image of Alexander-stained pollen grains from whole-mount filaments. Viable pollen accumulates red stain. Scale bar = 100 µm. (B) DAPI staining of mature pollen grain (tricellular stage). Scale bar = 50 µm. (C) Pollen tube germination. Scale bar = 200 µm.

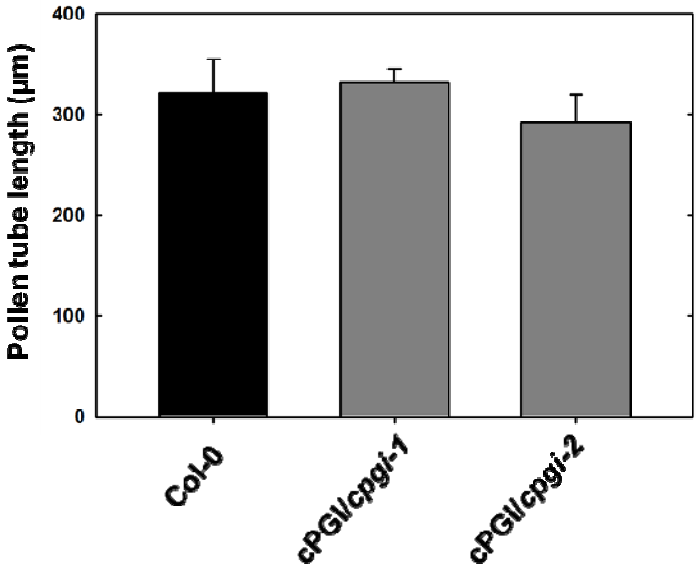

Figure 19: Pollen tube growth of Col-0 and heterozygous T-DNA lines after 16 h of incubation in dark at 28°C. Average ±SD, three replicates. No significant difference to wild-type (student's t-test, $\alpha \leq 0.05$).

3.12 Analysis of transmission efficiency of *cpgi* T-DNA mutants

As previously mentioned (section 3.1), *cPGI* expression is rather high in developing seeds and embryo. Therefore, to assess the female gametophytic and early embryo developing stages, the number of failed ovules (empty spots) in siliques of *cPGI/cpgi-1* and *cPGI/cpgi-2* plants was scored. Results indicate that the empty spaces are significantly higher in the T-DNA insertion lines opposed to wild-type siliques (Figure 20A, B). However, according to mendelian inheritance, 25% of failed ovules would be expected if failed ovules were the result of homozygous T-DNA embryo lethality. Yet, in this experiment, 11-21% of empty spaces were observed for *cpgi-2* and *cpgi-1*, respectively (Figure 20B), which is proposing the possible transmission of mutant allele to the next generation. Howden et al. (1998) introduced transmission efficiency as the percentage of number of heterozygote over the number of wild-type individuals in the progeny of reciprocal crosses. To investigate the transmission of the mutant allele through male and female gametophytes, reciprocal crosses of *cPGI/cpgi-1* and *cPGI/cpgi-2* with Col-0 were carried out. Results revealed the reduction of mutant allele transmission to at least 49% through female and 32% through the male gametophyte (Table 1).

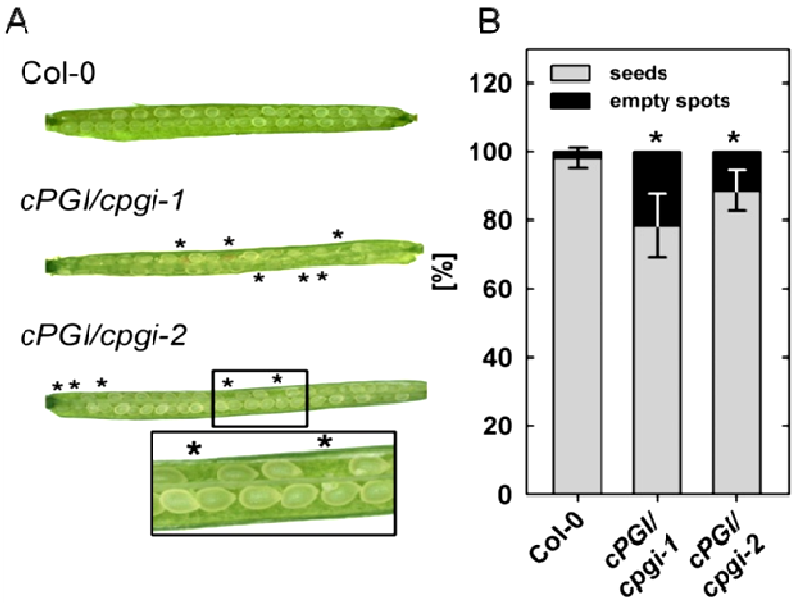

Figure 20: Effect of T-DNA insertion in ovule/seed development. (A) Representative siliques from wild-type, *cPGI/cpgi-1* and *cPGI/cpgi-2* plants. Asterisks mark empty spots in opened siliques. (B) Rate of seed abortion/development in *cPGI/cpgi* T-DNA mutants and wild-type. Average ±SD, n = 30. Asterisks indicate significant difference to wild-type (student's t-test, $\alpha \leq 0.01$).

Table 1: Progeny of crosses between wild-type and heterozygous *cpgi* T-DNA mutants was genotyped by PCR and transmission efficiency (TE) calculated as the ratio of number of heterozygous over number of wild-type plants. Transmission efficiency of the *cpgi* allele is strongly reduced through both male and female gametes.

		cpgi-1			cpgi-2		
F0 \ F1		cPGI/cPGI	cPGI/*cpgi*	TE [%]	cPGI/cPGI	cPGI/*cpgi*	TE [%]
cPGI/cPGI	cPGI/*cpgi*	102	33	32	94	21	22
cPGI/*cpgi*	cPGI/cPGI	33	11	33	120	59	49

3.13 Assessing T-DNA inheritance by analyzing the progeny of self-fertilizing heterozygous parent plants

Whether an expected and observed distribution match or differ can be analyzed by a chi-squared test. The chi squared value is calculated based on the equation $X^2 = \Sigma$ (Observed value – Expected value) ^{2} / (Expected value). The expected distribution of homozygous mutant, heterozygous and homozygous wild-type plants after self-fertilization was calculated based on the male and female transmission efficiencies for *cpgi-1* and *cpgi-2* determined from reciprocal crosses (Table 1; Figure 21A, B). Since the transmission efficiency through both male and female gametophyte was reduced but not abolished, the expectation would be to isolate 6% and 5.4% homozygotes in the progeny of heterozygous *cpgi-1* and *cpgi-2* mutants, respectively. However, despite of screening more than 300 plants, no homozygotes could be identified. These data indicate that in addition to the gametophytic effect of *cPGI* disruption, there is also an embryo lethal, zygotic effect. Hence, the observed partial transmission of the mutant allele to the next generation is likely the result of a combination of gametophytic and embryonic defects. Statistics based on the chi squared test (X^2) with two degrees of freedom revealed a significant difference in the distribution of the T-DNA allele when comparing the observed and expected T-DNA distribution (Table 2).

Table 2: Observed and expected genotype distribution in the progeny of self-fertilizing heterozygous *cpgi* plants. The expected genotype distribution was calculated based on the male and female transmission efficiencies for *cpgi-1* and *cpgi-2* according to Howden et al. (1998) as outlined in Fig. 20. *df*=2.

Ecotype		homozyg.	heterozyg.	Wild-type	total	χ^2	*p*
cpgi-1	obs.	0	148	156	304		
	exp.	18.2	112.5	173.3	304	31.2	$1.7\ 10^{-7}$
cpgi-2	obs.	0	159	146	305		
	exp.	16.5	119.6	168.9	305	32.6	$8.3\ 10^{-8}$

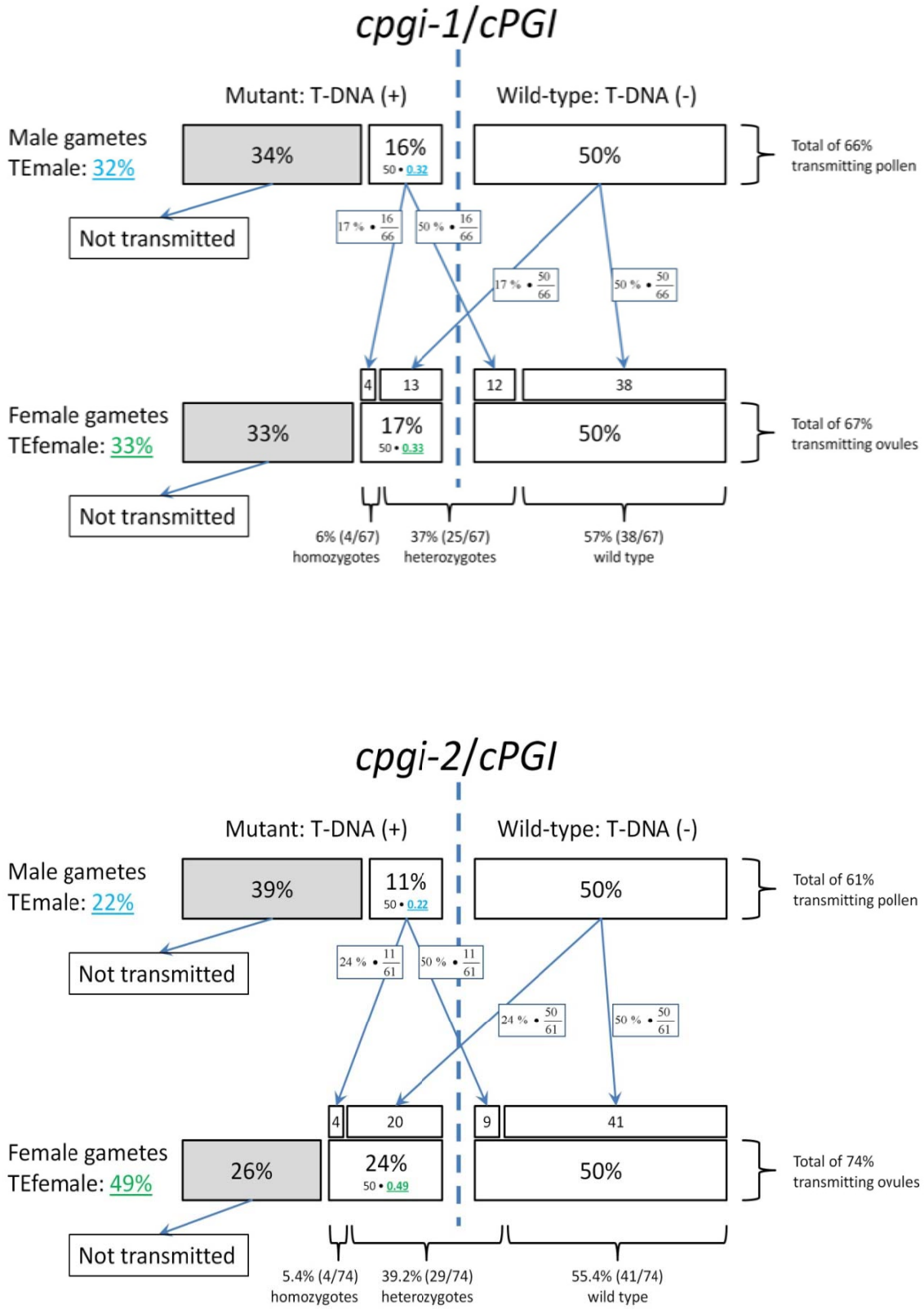

Figure 21: Illustration of expected and observed T-DNA inheritance in heterozygote mutants of (A) *cPGI/cpgi-1* and (B) *cPGI/cpgi-2* through male and female gametophytes.

3.14 Generation of complemented *cpgi* T-DNA lines

In an attempt to elucidate at which stage of development cPGI is more important and whether it is possible to obtain homozygous T-DNA mutants, cPGI cDNA was overexpressed in the background of *cPGI/cpgi-1* and *cPGI/cpgi-2* heterozygous mutants. Three different overexpressing lines were generated using three different promoters, the cauliflower mosaic virus 35S (CaMV 35S), the seed specific Unknown Seed Promoter (USP) and the Ubiquitin-10 (UBQ10) promoter. The idea of using different promoters originates from the fact that they drive expression during different periods of plant development. 35S and UBQ10 promoters are known to be expressed through all developmental stages. However, the 35S promoter has previously been reported to not being particularly active during male gametophyte development (Custers et al., 1999). The USP promoter is known to be expressed in developing seeds, five days after flowering and in cotyledons (Bäumlein et al., 1991; Ludewig K, 2013 unpublished). Transformed plants were selected for the presence of *cPGI* construct utilizing BASTA for plants harboring 35S/USP::cPGI::pAMPAT expression vectors and kanamycin and hygromycin selective plates for plants harboring the UBQ10::cPGI::pHygII-UT-c-term-Venus expression vectors. Through genotyping of selected T1 plants, homozygous T-DNA *cpgi* mutants for all constructs could be identified in the T1 generation (Figure 22; Table 3). However, isolating homozygous *cpgi-1/cpgi-1* using the 35S and pUSP promoters required genotyping of larger population (Table 3). Differences in the frequency of isolating homozygotes might be linked to the different insertion site of the T-DNA in *cpgi-1* (exon) or *cpgi-2* (intron) or the position of the complementation construct which might influence its expression (Figure 4A). On the other hand, the intronic mutation could be less effective than the exonic mutation. Using the genome-specific primer pairs designed to bind in exons only (fwd5/rev10) identified the presence of the introduced *cPGI* cDNA (Figure 22A). To prevent amplification of the complementation construct cDNA in genomic DNA PCR reactions, new intron specific primer pairs were designed for *cpgi-1* (fwd7/rev12) and *cpgi-2* (fwd2/rev9.5), respectively (Figure 22B, C).

Table 3: Homozygous *cpgi* T-DNA mutants isolated from over expressing lines with three different promoters including 35S, USP and UBQ10. The numbers in table show the ratio of homozygous *cpgi* T-DNA mutants over the total number of plants genotyped.

Mutant background / **Construct**	*cPGI/cpgi-1*	*cPGI/cpgi-2*
p35S::cPGI::pAMPAT	3 / 140	11 / 127
pUSP::cPGI::pAMPAT	5 / 176	7 / 70
pUBQ10::cPGI::pHygII-UT-c-term-Venus	9 / 70	11 / 105

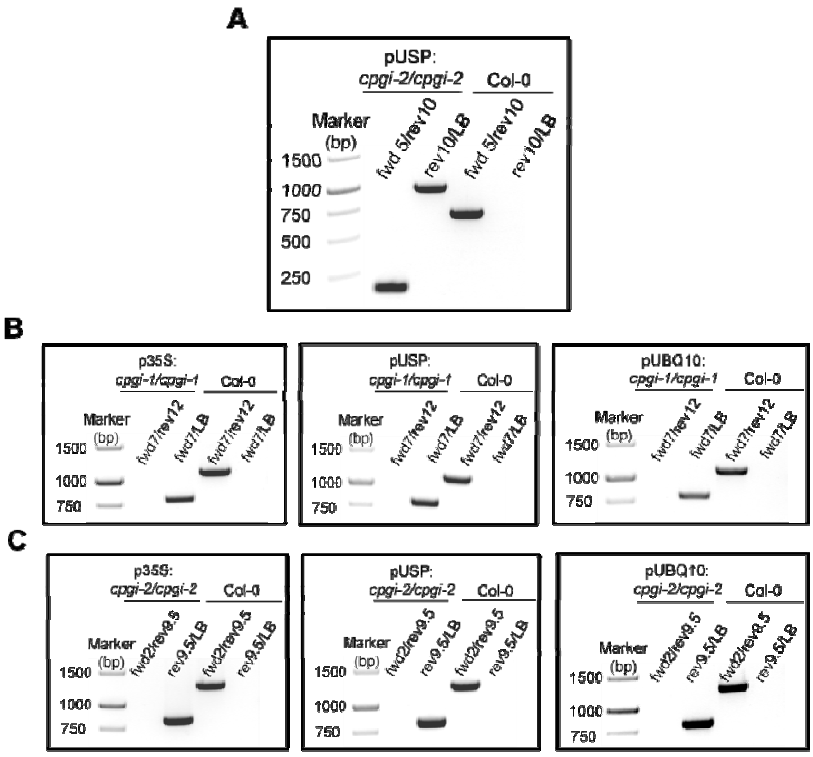

Figure 22: Detecting of homozygous T-DNA in cPGI overexpressing lines. (A) Identification of homozygous T-DNA lines using primer pairs designed on exon and amplification of cDNA introduced in the mutant background (B) Homozygous T-DNA *cpgi-1* and (C) Homozygous T-DNA *cpgi-2* over expressed with different promoters. The second primer pairs were designed on intron to prevent cDNA amplification and showing the homozygosity better.

Interestingly, except for two lines rescued by UBQ10 expression and homozygous for *cpgi-1*, all identified homozygous *cpgi* T-DNA mutants were sterile and failed to set seeds. Investigation of pollen from flowers of homozygous plants by Alexander staining revealed the absence of any pollen grains (Figure 23A). The pollen sacs of sterile mutants appeared shriveled and different from wild-type (Figure 23B). The

pistils of isolated, sterile homozygous mutants grew to a small silique with no seeds inside indicating that no egg cells could be fertilized (Figure 23C, D). However, a few seeds could still be gathered from each homozygote *cpgi* T-DNA but further genotyping identified them as cross pollinated ovules, because all of them were heterozygous for *cpgi*.

Apparently, complementation with the UBQ10 promoter could only produce sufficient *cPGI* transcript in a few but by far not all cases, since only two homozygotes for *cpgi-1* were fertile and produce seeds. This finding indicated that expression of *cPGI* using UBQ10 promoter was not sufficiently strong in all transformants, otherwise all homozygous *cpgi* mutants should have been fertile.

Subsequent analyses of total and cPGI activity in some lines of homozygous, over expressing plants, revealed that UBQ10 promoter activity was different in various lines with the two fertile lines showing the highest cPGI activity in leaves (Figure 24).

Figure 23: Phenotypes of mature homozygous *cpgi* T-DNA (*cpgi-1/cpgi-1*) plant overexpressing with p35S promoter. (A) Alexander staining of pollen grains as an indicator of pollen viability. (B) Shriveled pollen sacs. (C) Flower developments and a full grown silique derived from the pistil. (D) An opened silique with no fertilized seeds inside.

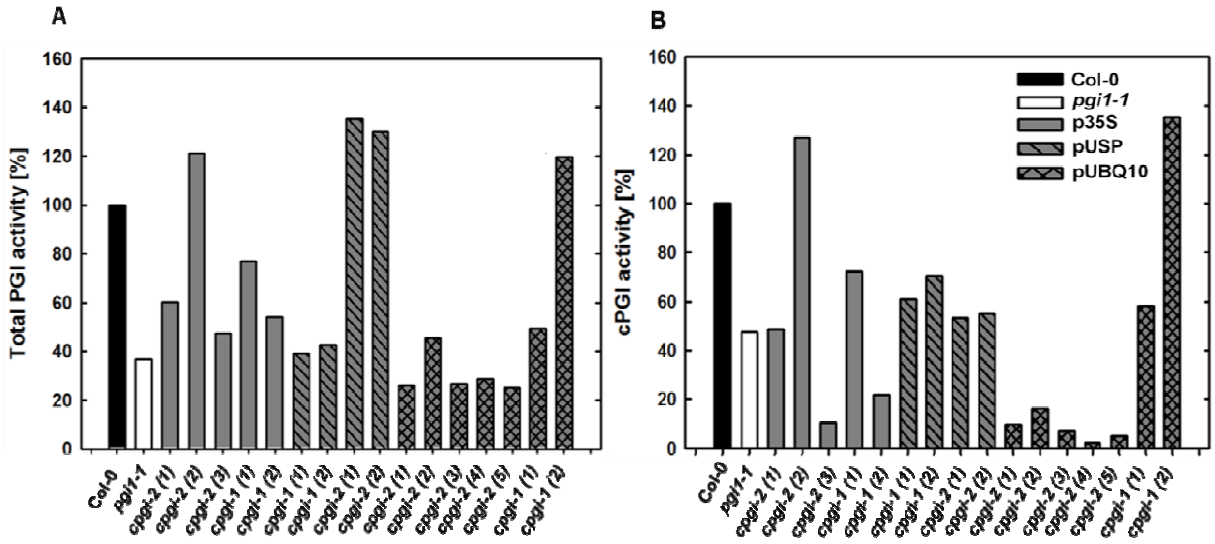

Figure 24: (A) Total PGI activity and (B) cytosolic PGI activity after heat inactivation of plastidic PGI in leaf extracts of various cPGI overexpressing lines of homozygous *cpgi-1* and *cpgi-2* mutants using three promoters of p35S, pUSP and UBQ10. Rates were normalized to total activity in leaf extracts from Col-0 wild-type.

To further prove that the sterility of homozygous *cpgi* T-DNA mutant is due to the lack of viable pollens, the flower pistil of a homozygous mutant was pollinated with the Col-0 wild-type pollen. Siliques of homozygous plants back-crossed with Col-0 pollen elongated almost normally and set viable seeds (Figure 25 A, B). Seedlings grown from these seeds were genotyped and all identified as heterozygotes as would be expected when back-crossing homozygous plants with wild-type pollen.

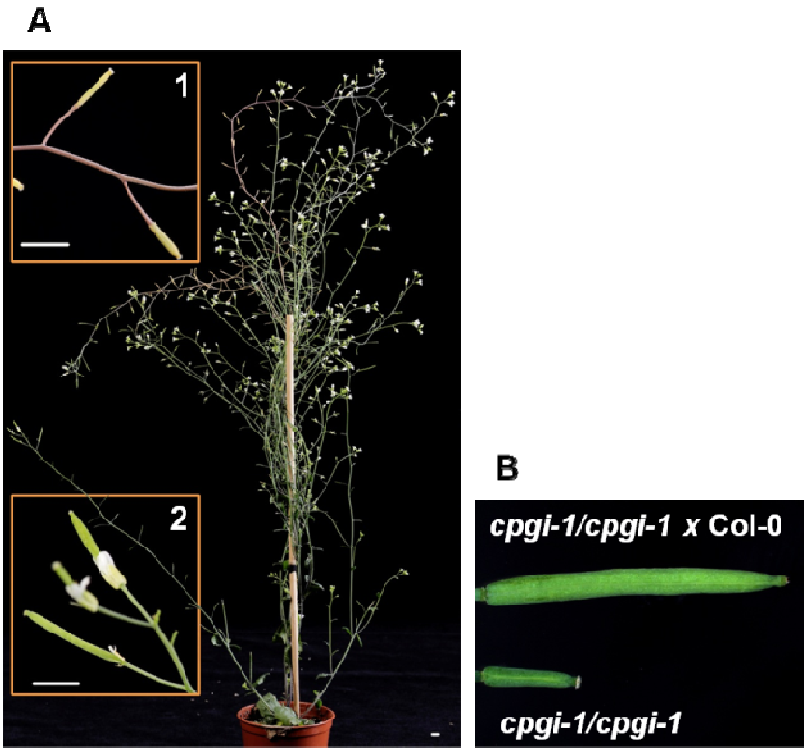

Figure 25: (A) The sterile homozygous *cpgi-1/cpgi-1* survived assisting the 35S promoter. (A_1) The mature sterile siligue developed from pistil (A_2) The mature fertile silique developed from a flower crossed with wild-type pollen. (B) Comparison of the size of fertile and sterile siliques developed from flowers pollinated with Col-0 and mutant pollens, respectively.

4. Discussion

The interconversion of fructose-6-phosphate into glucose-6-phosphate is mediated by phosphoglucoisomerases (PGI), enzymes involved in primary metabolism. The cytosolic PGI (cPGI) is crucial for sucrose production and carbon supply in the cytosol and provision of carbohydrates to sink tissues via sucrose long-distance transport. As such, the cPGI enzyme would play a key role in equilibration of carbohydrate turnover in plants and be important for overall plant vitality (Gibon et al., 2006; Usadel et al., 2008). This study investigated the impact of impaired *cPGI* function on mature amiRNA mutants and found that decreased cPGI activity can be tolerated by the plant but strongly affects nocturnal starch breakdown, the photosynthetic apparatus and plant reproduction.

4.1 *cPGI* function is essential for plant vitality

Screening of about 300 individual plants from a segregating seed population of heterozygous T-DNA insertion lines (*cPGI/cpgi*) did not identify any homozygous *cpgi* mutants (Figure 4B) indicating the imortance of cPGI in plant vitality. Egli et al. (2010) have characterized mutants with loss of cytosolic phosphoglucomutase (*cpgm*) and also failed to find homozygous double mutants in both cytosolic isoforms (*cpgm2/3*). In their study, they discovered failed gametophyte development as cause *cpgm2/3* lethality. As previously mentioned (1.1.2), cPGM enzymes act in concert with cPGI in sucrose production in plants. Hence, it was interesting to investigate this stage of development in heterozygous *cpgi* T-DNA mutants. Moreover, the *cPGI* expression level is relatively similar and high during male and female gametophyte development in the wild-type suggesting an important role of cPGI at this developmental stage (http://bar.utoronto.ca/efp/cgi-bin/efpWeb.cgi: Winter et al., (2007). All performed analyses on pollen grains, from viability and physiology (Figure 18A, B) to germination and pollen tube length (Figure 18C; 19) indicated normal pollen development on heterozygous *cpgi* parent plants.

It is known that pollen germination and pollen tube growth are energy consuming processes (Rounds et al., 2011). However, many heterotrophic tissues like pollen, ovules and early embryos are dependent to the autotrophic parental tissues

surrounding them. In this study, viability and physiology of pollen from heterozygous *cpgi* plants appeared not to be influenced by the T-DNA insertion. Since pollen grains are located and matured in the pollen sac, the surrounding heterozygous tapetum cells of the parent plant may provide sufficient metabolites and energy to ensure normal pollen development. However, when pollen are released and placed on the stigma, they will be on their own concerning metabolism and energy source. Moreover, the adequate substrates for ATP generation in the form of Glc6P and Fru6P generated from sucrose breakdown can be supplied from the parent plant to the mentioned tissues. In this respect, cPGI presence as the sole enzyme for reversible conversion of Glc6P and Fru6P is important for glycolytic activity and energy production. Therefore, reduced transmission of the mutant allele through both gametes (Table 1) might be due to the lack of energy supply resulting from cPGI deficiency.

In addition, the imbalance between the Glc6P and Fru6P pools in the cytosol could influence many biological processes and anabolic pathways in the plastid. Fru6P is either a substrate for the production of phosphoenolpyruvate (PEP), needed for plastidic shikimate pathway or a substrate for the pyruvate needed for fatty acid, amino acid and isoprenoid biosyntheses (Flügge et al., 2010). On the other hand, the required Glc6P can be imported into plastids of heterotrophic tissues by the GPT (Kammerer et al., 1998; Niewiadomski et al., 2005) and be utilized in plastidic oxidative pentosephosphate pathway (OPPP) to provide the reducing power (NADPH) for de novo fatty acid biosynthesis (Pleite et al., 2005). The OPPP also provides the phosphorylated C4 and C5 sugars essential for shikimate pathway and nucleotide biosynthesis, respectively. It is notable that the well-balanced fluxes of the glycolytic pathway and the OPPP is of high priority.

Taken together, first, the inability of mutant to balance phosphorylated hexose pools in cytosol (Glc6P and Fru6P) and second, the imbalance of fluxes in cytosol and plastid are causing the *cpgi* mutant defect at both gametophytic and zygotic stages.

4.2 Transmission efficiency of T-DNA insertion

Irregular T-DNA transmission to the next generation has been discussed previously (Feldmann et al., 1997; Howden et al., 1998) and can be calculated as the

transmission efficiency and allows estimation of the percentage of gametes transmitting the mutant allele (Howden et al., 1998). Partial or absent transmission of the T-DNA might be the result of non-vital female gametophytes (Thushani et al., 2011), male gametophytes (Park et al., 1998; Procissi et al., 2001) or/and zygotes, i.e. embryos (Meinke and Sussex 1979; Candela et al., 2011).

The T-DNA segregation of both self-fertilizing heterozygous *cpgi* lines represents a distribution of 1:1 (*cpgi*/cPGI:cPGI/cPGI) rather than the expected 1:2:1 (*cpgi*/*cpgi* : *cpgi*/cPGI : cPGI/cPGI) in a normal condition (Table 2). Moreover, by the lethality of homozygous *cpgi* T-DNA mutants, we should expect a ratio of 0:2:1. The only time that a ratio of 1:1 can be expected is when one of the gametophytes is completely defective. This event was not the case in the current study, since we have a partial transmission of mutant allele through both male and female gametophytes (Table 1). The reduced transmission is an indicator of partially defective gametophytic stages. The calculation of the *cpgi* T-DNA mutant allele inheritance in self-fertilizing heterozygous *cpgi* mutants based on the reduced transmission is depicted as a cartoon in Figure 21. These numbers reveal that theoretically 5.4 – 6 % of homozygous *cpgi* T-DNA mutants would be expected. However, no homozygous plant has been identified from a screening population of more than 300 plants, strongly indicating that homozygous *cpgi* T-DNA mutants aside from being defective in gametophytes are embryo lethal. However, according to the percentage of failed ovules and failed homozygous mutants, one should expect a percentage of more than 25% (mendelian inheritance), e.g. for *cpgi-1*; (33% + 4%) and for *cpgi-2*; (26% + 4%) (Figure 21). Yet, the percentage of empty spaces within the siliques of mutant lines was even less than 25% (11-21%) (Figure 20). Therefore, the theoretically calculated numbers for failed seeds do not exactly match the observed percentage of empty spots in siliques of heterozygous *cpgi* mutants.

There are several possible explanations for this discrepancy. There might be additive effects in place resulting from overlaying impacts on gametophyte and zygote viability which could distort the observed percentage of failed seeds.

In addition, often the microscopic view into siliques may not entirely reflect the *in vivo* situation. After having been opened with a scalpel, particularly small undeveloped seeds may be lost or concealed by damaged tissue. Thus, there is the possibility that failed seeds have been overlooked and not been recognized as such when counting

developed and undeveloped seeds in opened siliques leading to unintentional bias towards developed seeds.

A third explanation could be linked to the observed transmission efficiencies. If the observed transmission efficiency was underestimated, i.e. it is actually higher than determined, the expected percentage of failed ovules would decrease and could approach values such as those observed. Underestimation of transmission efficiency could result from a wild-type contamination either by accidentally using pollen of a wild-type plant for reciprocal crosses or pollinating a presumed heterozygous *cpgi* plant that in fact is a wild-type plant. In both cases wild-type plants would be over-represented in the F1 generation resulting in underestimation of the transmission efficiency, i.e. the more strongly reduced transmission efficiency than in reality. An experimental error like this may happen, for example, if the PCR based genotyping of plants used for reciprocal crosses provided faulty results.

In reality, it may be the sum of both, the underestimation of empty spots in siliques and the underestimation of transmission efficiencies that has led to the discrepancy between percentages of observed and expected failed seeds in siliques of heterozygous *cpgi* plants.

4.3 Increased starch and heteroglycan contents as result of the absent cPGI activity

Decreased cPGI activity through expression of the artificial micro RNAs against *cPGI* mRNA led to starch excess in leaves of mutant plants at all time points during a day/night cycle, most prominently at the end of the night (Figure 12; 14). A link between the activity of a cytosolic enzyme and the chloroplastidic process of starch biosynthesis is unexpected at first glimpse. However, it may at the same time be conceivable since other studies investigating cytosolic processes such as sucrose export from mesophyll cells (Gottwald et al., 2000; Srivastava et al., 2008) or turnover of heteroglycans via disproportioning enzyme (DPE2) (Chia et al., 2004; Lu and Sharkey, 2004) also reported starch excess in loss-of-function mutants. DPE2 facilitates the transient incorporation of maltose derived-glucose into cytosolic heteroglycans and is acting upstream of cPGI in the cytosol. Thus impairment of *cPGI* function could affect starch metabolism similar to loss of *DPE2* (Figure 13).

Besides, it has previously been shown that the heteroglycan monomer composition is altered in leaves of *dpe2* mutants (Fettke et al., 2006; Malinova et al., 2013). Similar to *dpe2* mutants, amiR1-*cpgi* plants showed a significant increase of the glucose monomer content of heteroglycans (Figure 15B). This accumulation may be explained by the lack of cPGI enzyme activity and thus decreased heteroglycan glucose moiety turnover for sucrose biosynthesis. Hence, because of the decreased sucrose synthesis ability, transitory starch breakdown appears to be reduced leading to the observed starch excess phenotype. Collectively, the data suggest that lack of cPGI enzyme activity does not only affect the turnover and metabolism of starch breakdown products in the cytosol but also starch degradation in chloroplasts itself. In consequence, this would require some so far unidentified mechanism feeding back from the cytosol to chloroplasts.

4.4 Alteration of photosynthetic parameters and growth in amiR-*cpgi* plants

Absence of cPGI activity also led to other alterations in plants, e.g. in regards to photosynthesis but also in regards to plant growth. According to PAM measurements of dark-adapted plants, amiR-*cpgi* mutants displayed a clearly increased non-photochemical quench coefficient (q_N) but a decreased photochemical quench coefficient (q_P) and electron transport rate (ETR) (Figure 9C; 11). In contrast to amiR-*cpgi* plants, q_N in *dpe2* mutant lines did not differ from the corresponding Wassilewskija wild-type (Figure 10).

Non-photochemical quenching and chlorophyll fluorescence are employed by chloroplasts as protective system to get rid of excess energy and avoid damage to surrounding photosynthetic membranes. A balanced content of triose phosphates and inorganic phosphate (Pi) in the cytosol and the chloroplast helps the plant to maintain high photosynthetic efficiency. In this sense, chloroplastidic photophosphorylation may be impaired when Pi is in limited supply in the stroma because of decreased sucrose formation in the cytosol. In other words, a too fast or too slow production of sucrose in the cytosol may cause the photosynthesis machinary to be negatively impacted (Strand et al., 2000). The decreased sucrose content in amiR-*cpgi* mutants at the end of the night (Figure 15A; 16) may lead to Pi

shortage in chloroplasts for the generation of glycerate 3P (3-PGA) and ATP (Stitt, 1986; Stitt et al., 1987) along with imbalanced carbon metabolism in the cytosol and chloroplasts, i.e. sucrose and starch production, respectively (Stitt, 1996). Thus, a possible Pi shortage in the chloroplast may finally cause a lower ETR in amiR-*cpgi* plants compared to wild-type (Figure 9C; 11) during PAM measurement. The q_P and ETR, however, finally approached wild-type levels at the end of the induction time, i.e. after the initial phase, photosynthesis worked quite normal. This could be due to the partial starch degradation to pick up after transition into the light and deliver substrate for sucrose biosynthesis (Glc6P, Glc1P). Once these substrates are available, the sucrose synthesis might run quite normal as seen in wild-type like steady state levels of sucrose in leaves during the day (light period). Along with the change in q_N, the q_P is decreased indicating that the primary electron acceptor Q_A is existing mainly in the reduced state, which in turn affects the ETR and reduces ATP formation in photosystem II.

However, q_N and q_P were unaltered compared to wild-type in *dpe2* mutants (Figure 10) while these mutants also showed a starch excess phenotype. This difference to amiR-*cpgi* plants may be attributed to the fact that DPE enzyme activity occurs mainly during the night period when starch-derived maltose needs to be metabolized; i.e. an impact of the absence of DPE activity on photosynthesis is not expected.

In brief, slowed-down sucrose biosynthesis during dark to light transition in amiR-*cpgi* plants could be rate limiting for photosynthetic activity. In our PAM analysis of amiR-*cpgi* plants photosynthetic activity and electron transport rate gradually reached wild-type level during light induction curves supporting this interpretation (Figure 9C; 11).

Moreover, the growth rate and fresh weight of amiR-*cpgi* mutants were reduced (Figure 7A, B), but mutant plants could eventually develop into normal plants and reproduce. Reduction in sucrose tissue content due to low activity of cPGI in *Clarkia* (Neuhaus et al., 1989), down regulated the TPT transporter in potato (Heineke et al., 1994) or decreased expression of cytosolic fructose 1,6-bis phosphatase in potato and *Flavaria* (Zrenner et al.,1996; Sharkey et al., 1992) were consistent with current study in which lack of sucrose production leads to alteration of starch biosynthesis and less influence on photosynthetic rate and growth.

4.5 Lack of cPGI activity leads to impaired sucrose biosynthesis at the end of the night

In spite of absent cPGI activity in amiR-*cpgi* lines (Figure 6B), measurements of mature leaves revealed considerable amounts of sucrose at different time points during the day/night cycle which were comparable with wild-type levels (Figure 15A; 16). However, a significant reduction in sucrose content was observed at the end of the night in amiR-*cpgi* plants.

In amiR-*cpgi* plants, Fru6P, one of the substrates for sucrose biosynthesis, can be generated via the regular 'day path' of carbon from chloroplast-exported triose phosphate during the day (Figure 26). On the other hand, the demand for Glc6P, the second substrate for sucrose biosynthesis, cannot be met by the 'day path' of carbon since Glc6P cannot be generated from Fru6P in amiR-*cpgi* plants. Instead, Glc6P could be derived from breakdown of transitory starch during the day, i.e. the 'night path' of carbon (Figure 26). The products exported from chloroplasts during starch breakdown are glucose and maltose. Glucose can be supplied in the cytosol either by direct export of glucose through the glucose transporter pGlcT (Weber et al., 2000). Moreover, maltose can be exported from chloroplasts to the cytosol by the envelope-localized protein maltose exporter MEX1 (Niittylä et al., 2004) and results in production of maltose- and heteroglycan-derived glucose in the cytosol with the help of DPE2 (Chia et al., 2004; Lu and Sharkey, 2004) and cytosolic glucan phosphorylase Pho2 (Figure 26).

In addition, Fettke et al. (2011) could show that Glc1P can be directly transported into isolated Arabidopsis protoplasts and chloroplasts offering a third pathway for glucose provision to the cytosol which could be a shortcut for sucrose biosynthesis during the day without the necessity for starch breakdown in amiR-*cpgi* plants. Glucose can be further converted to Glc1P through action of hexokinase and cPGM. Glc1P is then metabolized to UDP-Glc, the substrate for sucrose phosphate synthase.

It has been shown previously that partial starch degradation during the day can be a compensatory mechanism in mutants impaired in the triose phosphate/ phosphate translocator (*tpt-1* mutant, Schneider et al., 2002; Walters et al., 2004). On the other hand, the severe growth retardation in amiR-*cpgi* mutant in the background of the

starch free mutants *pgi1-1* and *adg1-1* (Figure 17) was consistent with the research of Heinrichs et al. (2012) in which the *tpt-1* mutant revealed a dwarf growth phenotype in the absence of starch. The strong decrease in sucrose content at the end of the night was in opposite to the situation during the day which did not reveal any differences in sucrose content between wild-type and amiR-*cpgi* palnts (Figure 15A; 16). Apparently, sucrose biosynthesis is more of a problem during the night in amiR-*cpgi* plants. During the night, the supply of Fru6P is not possible neither by the action of the cPGI enzyme nor through triose phosphates (TP), since the enzyme fructose 1,6-bisphosphatase is inactive (Cseke et al., 1982; Stitt, 1990). The latter enzyme activity is strictly relying on the concentration of the photoassimilated TP. It means that in the absence of photosynthesis during the night, the concentration of TP drops to a low level while at the same time the regulatory metabolite fructose 2, 6-bisphosphate accumulates. Both effects lead to an efficient inactivation of the fructose 1,6-bisphosphatase (Stitt et al., 1985). Therefore, the insufficient energy supply during the night and the inability to maintain a well-balanced carbon flux (Ludewig and Flügge, 2013), might be the cause for the low growth rate observed for amiR-*cpgi* plants (Figure 7; 8) and other mutants defective in carbohydrate metabolism such as *pgi1-1*, *pgm* and *adg1* (Yu et al., 2000), *suc2* and *sweet1sweet2* (Gottwald et al., 2000; Chen et al., 2012) and starch excess mutant *sex1* (Rasse and Tocquin, 2006; Streb et al., 2012). However, all these mutants seem to grow normally later. The more pronounced growth phenotype of amiR-*cpgi* plants under short-day condition (longer night period) was an additional hint for the greater importance of cPGI enzyme activity during the night compared to the day.

4.6 Rescue of the embryo lethality and gametophytic phenotype of *cpgi* T-DNA mutants by complementation

In order to recover homozygous T-DNA *cpgi* mutants, complementation analysis was attempted using three different promoters expressing the *cPGI* cDNA (see 3.14). The overexpressing lines were generated in order to isolate homozygous T-DNA mutants and to gain insight into which stage of plant development is most dependent on cPGI enzyme activity. After genotyping of plants positively selected from the T1 generation, homozygous *cpgi* T-DNA insertion mutants could be identified with all of

the promoters used (p35S, pUSP, pUBQ10) for both *cpgi-1* and *cpgi-2* (Table 3; Figure 22). However, after flowering, it became obvious that all homozygotes were self-sterile and not able to reproduce, unless *cPGI* expression was driven by pUBQ10 for which two lines of *cpgi-1/cpgi-1* were fertile. It seems that cPGI activity resulting from expression of the employed promoters is sufficient to ensure survival of homozygous mutants that resulted from fertilization on heterozygous plants. However, expression of the cPGI transgene driven by the CaMV35S or pUSP promoter was apparently insufficient during gametogenesis and embryogenesis to produce pollen. As long as mutant pollen grains can be produced on heterozygous parent plants, they will be vital and functional which is not the case for homozygous parent plants which are defective in pollen formation. In sterile homozygous plants, the silique stopped developing as a result of lacking fertilization which was caused by the absence of pollen in their anthers. Investigating homozygous mutant's flowers in detail revealed that anthers appeared shriveled and filaments did not elongate beyond the edge of stigma (Figure 23B). Mutants with anthers devoid of pollen have been generated and studied several times in approaches using T-DNA and EMS induced mutations defective in anther morphology or/and microspore formation (Sanders et al., 1999; Chaudhury et al., 1994). Sanders et al. (1999) introduced the *POLLENLESS3* gene expressed between the phase of microsporocyte formation and microsporogenesis prior to miosis. T-DNA *pollenless 3-2* mutants defective in sporophytically acting genes affecting the cell layers surrounding locules and its allele is reduced to 129 amino acids similar to EMS *ms5-1*mutant introduced by Chaudhury et al. (1994) in which all anther cells were affected at early stage of anthesis. These mutant plants were also not able to produce pollen and anthers were flattened and placed in a lower level of stigma. On the other hand, crossing of otherwise sterile homozygous mutants using wild-type pollen was successful indicating that the female gametophyte is developing better in these plants (Figure 25B).

Sucrose as a major transport form of carbon plays a critical role throughout the cell cycle and cell division in plants (Riou-Khamlichi et al., 2000; Patrick et al., 2013). Moreover, sucrose has a major effect on androgenesis. The anther nutritive cell layer (tapetum) and differential expression of many genes involved in anther development influence the microsporogenesis extensively (Goldberg et al., 1993; Tripathi and Singh, 2008). For example, *in vitro* cultivation of anther and pollen from *Lilium*

longiflorum was carried out by Clement and Audran, (1995) to investigate the anther maturation phase under different sucrose concentration. It revealed that the middle layer of the anther wall is important for transporting sucrose and other sugars to the developing pollen. Any mutations in that sporophytic layer influence the gametophytic tissue like pollen. Additionally, Pressman et al. (2012) reported that sucrose is the first and main soluble sugar participating at the late stage of pollen development in tomato plant. Besides, sucrose is a fundamental element for acetyl-CoA production resulting from pyruvate oxidation and Krebs cycle. Pyruvate is the final product of glycolysis. In addition, sporopollenin as a main component of the exine, the lipid-rich outer layer of the pollen grain wall, is known to be enriched in fatty acids and phenolic components (Blackmore et al., 2007). Therefore, lack of sucrose impacts acetyl-CoA generation and could consequently affect the fatty acid composition of the exine. It seems that in homozygous *cpgi* T-DNA mutants defective in carbohydrate metabolism during pollen development, insufficient carbon supply leads to a pollen-less phenotype and male sterility.

Above all, the fertile homozygous mutant *cpgi-1/cpgi-1* utilizing UBQ10-driven expression of *cPGI* indicates the importance of cPGI enzyme activity particularly during pollen development since pUBQ10 is the only of the three promoters used known to be active during all developmental stages (Norris et al., 1993). However, pUBQ10-driven expression also has been reported to be moderate and not evenly high in all tissues of Arabidopsis (Grefen et al., 2010; Norris et al., 1993). Notably, analysis of total PGI and cPGI enzyme activity in different homozygous lines of *cpgi-1* and *cpgi-2* have indicated that full male fertility is achieved in those lines, which are driven by UBQ10, is dependent on high expression of *cPGI*, i.e. promoter activity (Figure 24). We analyzed the expression of *cPGI* in mature leaves of complementation lines and detected considerable differences in expression between different lines (Figure 24). It may be assumed that lines showing a higher *cPGI* expression in mature leaves also exhibit a higher transgenic expression during pollen generation which in turn leads to full male fertility in those lines.

6. Conclusion

The cytosolic phosphoglucoisomerase (cPGI) is involved in sucrose biosynthesis in source tissues, while its lack of activity in heterotrophic tissues remains elusive. However, cPGI activity is vitally important for plants since no homozygous T-DNA lines could be isolated in this study. In order to investigate the impact of the functional loss of cPGI activity, we generated artificial micro RNA-plants (amiRNA) and analyzed five independent lines. Although cPGI activity was completely lost, these plants were viable but reduced in growth, leaf area and fresh weight compared to the wild-type. Furthermore, *cpgi* plants showed higher glucose contents of cytosolic heteroglycans, excess starch in chloroplasts and lower sucrose content in mature leaves at the end of the night. Taken together, we ended up to the final model in which starch accumulates excessively in amiR-*cpgi* leaf cell during the night in comparison with wild-type mainly due to decreased capacity to convert starch breakdown products into exportable sucrose in the cytosol. Moreover, during the day partial starch breakdown to fuel sucrose biosynthesis may help amiR-*cpgi* mutants to survive because our results revealed that the inability of transitory starch formation severely impairs viability of amiR-*cpgi* plants on soil (Figure 25). However, this metabolic adaptation slows down the ability to form sucrose after dark to light transition explaining the observed impact of impaired cPGI activity on photosynthesis.

Analysis of two individual heterozygous *cpgi* T-DNA lines showed that transmission efficiency of mutant alleles was impaired but not abolished through both male and female gametophytes. This finding reveals a decisive role of cPGI at the stage of gametophyte development along with embryo lethality, since no expected homozygots could be isolated. Finally, the homozygous T-DNA mutant could be partially rescued by complemention using three different promoters (p35S, pUSP, pUBQ10). Since complemented lines were only male fertile when *cPGI* expression was driven by the truly ubiquitously active UBQ10 promoter it can be concluded that cPGI is essential during sporogenesis.

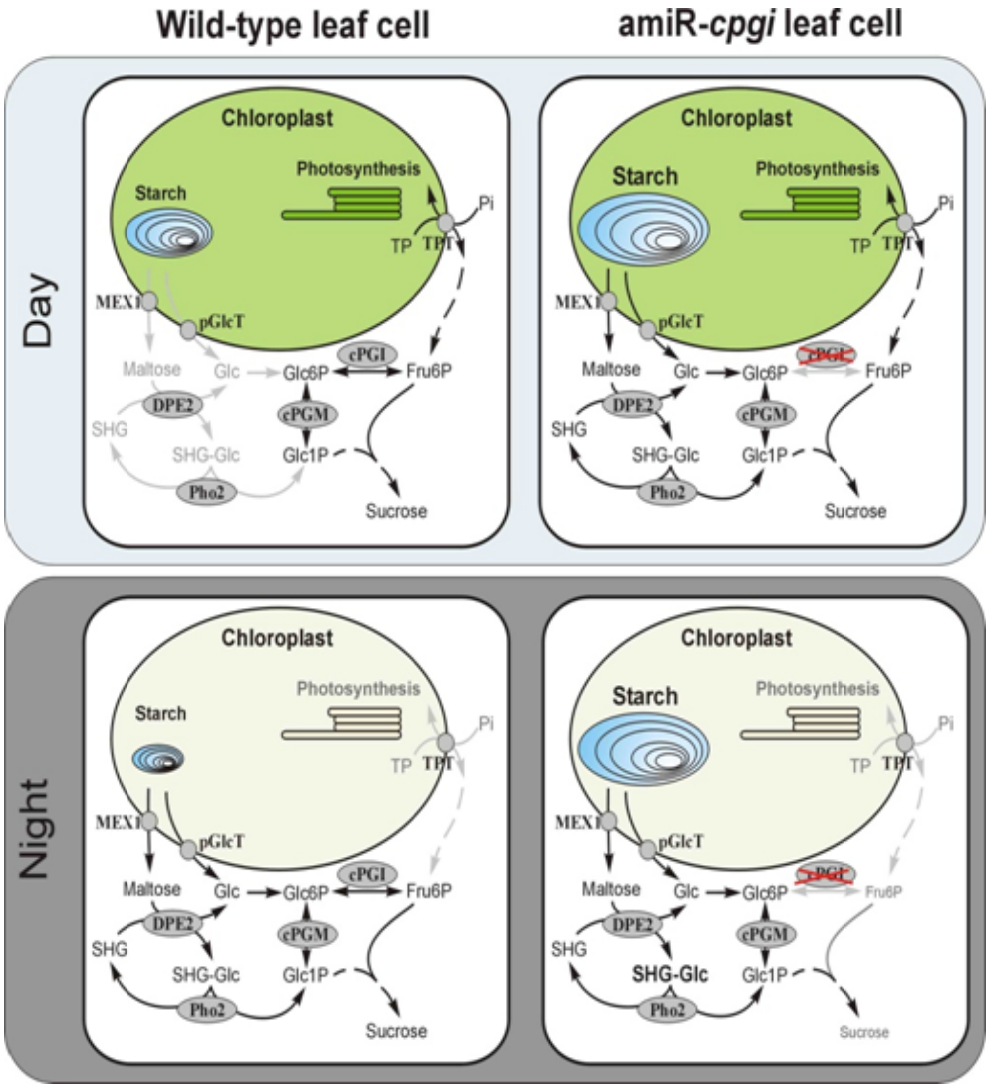

Figure 26: Model of cPGI involvement in sucrose and starch metabolism during the day and night cycles in amiR-*cpgi* leaf cells in compare to wild-type plant. MEX1: maltose exporter 1; pGlcT: plastid glucose transporter; TPT: triose phosphate/phosphate translocator; DPE2: disproportionating enzyme 2; Pho2: cytosolic phosphorylase 2; cPGM: cytosolic phosphoglucose mutase; SHG: soluble heteroglycans.

7. References

Alexander MP (1969) Differential staining of aborted and nonaborted pollen. Stain Technol 44: 117-122

Alonso JM, Stepanova AN, Leisse TJ, Kim CJ, Chen H, Shinn P, Stevenson DK, Zimmerman J, Barajas P, Cheuk R et al. (2003) Genome-wide insertional mutagenesis of *Arabidopsis thaliana*. Science 301: 653-657

Baud S, Lepiniec L (2009) Regulation of de novo fatty acid synthesis in maturing oilseeds of Arabidopsis. Plant Physiol Biochem 47: 448-455

Bäumlein H, Boerjan W, Nagy I, Bassüner R, Van Montagu M , Inze D, Wobus U (1991) A novel seed protein gene from *Vicia labs* is developmentally regulated in transgenic tobacco and *Arabidopsis* plants. Mol Gen Genet 225: 459-467

Bernier G, Havelange A, Houssa C, Petitjean A, Lejeune P (1993) Physiological signals that induce flowering. Plant Cell 5: 1147-1155

Blackmore S, Wortley AH, Skvarla JJ, Rowley JR (2007) Pollen wall development in flowering plants. New Phytol 174: 483-498

Boavida LC, McCormick S (2007) Technical advance: Temperature as a determinant factor for increased and reproducible *in vitro* pollen germination in *Arabidopsis thaliana.* Plant J 52:570-582

Brotman Y, Riewe D, Lisec J, Meyer RC, Willmitzer L, Altmann T (2011) Identification of enzymatic and regulatory genes of plant metabolism through QTL analysis in *Arabidopsis*. Plant Physiol 168: 1387-1394

Candela H, Perez-Perez JM, Micol JL (2011) Uncovering the post-embryonic functions of gametophytic- and embryonic-lethal genes. Trends Plant Sci 16: 336-345

Caspar T, Huber SC, Somerville C (1985) Alterations in growth, photosynthesis, and respiration in a starchless mutant of *Arabidopsis thaliana* (L.) deficient in chloroplast phosphoglucomutase activity. Plant Physiol 79: 11-17

Chaudhury AM, Lavithis M, Taylor PE, Craig S, Singh MB, Signer ER, Knox RB, Dennis ES (1994) Genetic control of male fertility in *Arabidopsis thaliana:* structural analysis of premeiotic developmental mutants. Sex Plant Reprod 7: 17-28

Chen LQ, Qu XQ, Hou BH, Sasso D, Osorio S, Fernie AR, Frommer WB (2012) Sucrose efflux mediated by SWEET proteins as a key step for phloem transport. Science 335: 207-2011

Chia T, Thorneycroft D, Chapple A, Messerli G, Chen J, Zeeman SC, Smith SM, Smith AM (2004) A cytosolic glucosyltransferase is required for conversion of starch to sucrose in *Arabidopsis* leaves at night. Plant J 37: 853-863

Cho MH, Lim H, Shin DH, Jeon JS, Bhoo SH, Park YI, Hahn TR (2011) Role of the plastidic glucose translocator in the export of starch degradation products from the chloroplasts in *Arabidopsis thaliana*. New Phytol 190: 101-112

Clement C, Audran JC (1995) Anther wall layers control pollen sugar nutrition in *Lilium.* Protoplasma 187:172-181

Clough SJ, Bent AF (1998) Floral dip: a simplified method for *Agrobacterium*-mediated transformation of *Arabidopsis thaliana*. Plant J 16: 735-743

Custers JBM, Snepvangers SCHJ, Jansen HJ, Zhang L, Lookeren Campagne MM (1999) The 35S-CaMV promoter is silent during early embryogenesis but activated during nonembryogenic sporophytic development in microspore culture. Protoplasma 208: 257-264

Cseke C, Weeden NF, Buchanan BB, Uyeda K (1982) A special fructose bisphosphate functions as a cytoplasmic regulatory metabolite in green leaves. Proc Natl Acad Sci USA 79: 4322-4326

Dalchau N, Baek SJ, Briggs HM, Robertson FC, Dodd AN, Gardner MJ, Stancombe MA, Haydon MJ, GB, Gonçalves JM, Webb AAR (2011) The circadian oscillator gene GIGANTEA mediates a long-term response of the Arabidopsis thaliana circadian clock to sucrose. PNAS 108: 5104-5109

Egli B, Kölling K, Köhler C, Zeeman SC, Streb S (2010) Loss of cytosolic phosphoglucomutase compromises gametophyte development in *Arabidopsis*. Plant Physiol 154: 1659-1671

Feldmann KA, Coury DA, Christianson ML (1997) Exceptional segregation of selectable marker (Kan^R) in Arabidopsis identifies genes important for gametophytic growth and development. Genetics 147: 1411-1422

Fettke J, Eckermann N, Poeste S, Pauly M, Steup M (2004) The glycan substrate of the cytosolic (Pho 2) phosphorylase isozyme from *Pisum sativum* L.: identification, linkage analysis and subcellular localization. Plant J 39: 933-946

Fettke J, Eckermann N, Tiessen A, Geigenberger P, Steup M (2005) Identification, subcellular localization and biochemical characterization of water-soluble heteroglycans (SHG) in leaves of *Arabidopsis thaliana* L.: distinct SHG reside in the cytosol and in the apoplast. Plant J 43: 568-585

Fettke J, Chia T, Eckermann N, Smith A, Steup M (2006) A transglucosidase necessary for starch degradation and maltose metabolism in leaves at night acts on cytosolic heteroglycans (SHG). Plant J 46: 668-684

Fettke J, Malinova I, Albrecht T, Hejazi M, Steup M (2011) Glucose-1-phosphate transport into protoplasts and chloroplasts from leaves of *Arabidopsis*. Plant Physiol 155: 1723-1734

Flügge UI, Häusler RE, Ludewig F, Gierth M (2010) The role of transporters in supplying energy to plant plastids. J Exp Bot 62: 2381-2392

Gibon Y, Pyl ET, Sulpice R, Lunn JE, Hohne M, Gunther M, Stitt M (2009) Adjustment of growth, starch turnover, protein content and central metabolism to a decrease of the carbon supply when *Arabidopsis* is grown in very short photoperiods. Plant Cell Environ 32: 859-874

Gibon Y, Usadel B, Blaesing OE, Kamlage B, Hoehne M, Trethewey R, Stitt M (2006) Integration of metabolite with transcript and enzyme activity profiling during diurnal cycles in *Arabidopsis* rosettes. Genome Biol 7: R76

Gibson K, Park JS, Nagai Y, Hwang SK, Cho YC, Roh KH, Lee SM, Kim DH, Choi SB, Ito H, Edwards GE, Okita TW (2011) Exploiting leaf starch synthesis as a transient sink to elevate photosynthesis, plant productivity and yields. Plant Sci 181: 275-281

Goldberg RB, Beals TP, Sanders PM (1993) Anther development: basic principles and practical applications. The Plant Cell 5: 1217-1229

Gottlieb LD (1977) Evidence for duplication and divergence of the structural gene for phosphoglucoisomerase in diploid species of *Clarkia.* Genetics 86: 289-307

Gottlieb LD, Higgins RC (1984) Evidence from subunit molecular weight suggests hybridization was the source of the phosphoglucose isomerase gene duplication in *Clarkia.* Theor Appl Genet 68: 369-373

Gottwald JR, Krysan PJ, Young JC, Evert RF, Sussman MR (2000) Genetic evidence for the in planta role of phloem-specific plasma membrane sucrose transporters. Proc Natl Acad Sci USA 97: 13979-13984

Graf A, Smith AM (2011) Starch and the clock: the dark side of plant productivity. Trends Plant Sci 16: 169-175

Grefen C, Donald N, Hashimoto K, Kudla J, Schumacher K, Blatt MR (2010) A ubiquitin-10 promoter-based vector set for fluorescent protein tagging facilitates temporal stability and native protein distribution in transient and stable expression studies. Plant J 64: 355-365

Hansen T, Schlichting B, Felgendreher M, Schönheit P (2005) Cupin-type phosphoglucose isomerases (Cupin-PGIs) constitute a novel metal-dependent PGI family representing a convergent line of PGI evolution. J Bacteriol 187: 1621-1631

Heineke D, Kruse A, Flügge U-I, Frommer WB, Riesmeier JW, Willmitzer L, Heldt HW (1994) Effect of antisense repression of the chloroplast triose-phosphate translocator on photosynthetic metabolism in transgenic potato plants. Planta 193: 174-180

Heinrichs L, Schmitz J, Flügge UI, Häusler RE (2012) The mysterious rescue of *adg1-1*/*tpt-2* - an *Arabidopsis thaliana* double mutant impaired in acclimation to high light- by exogenously supplied sugars. Front Plant Sci 3: 265-doi: 10.3389/fpls.2012.00265

Herbert M, Schnarrenberger C (1982) Purification and subunit structure of glucosephosphate isomerase 2 from spinach leaves and immunochemical comparison with other isomerases. Archive Biochem Biophys 217: 452-459

Howden R, Park SK, Moore JM, Orme J, Grossniklaus U, Twell D (1998) Selection of T-DNA-tagged male and female gametophytic mutants by segregation distortion in *Arabidopsis*. Genetics 149: 621-631

Ito J, Batth TS, Petzold CJ, Redding-Johanson AM, Mukhopadhyay A, Verboom R, Meyer EH, Millar AH, Heazlewood JL (2011) Analysis of the *Arabidopsis* cytosolic proteome highlights subcellular partitioning of central plant metabolism. J Proteome Res 10: 1571-1582

Izumi M, Hidema J, Makino A, Ishida H (2013) Autophagy contributes to nighttime energy availability for growth in *Arabidopsis*. Plant Physiol 161: 1682-1693

Jones TWA, Pichersky E, Gottlieb LD (1986a) Enzyme activity in EMS-induced null mutations of duplicated genes encoding phosphoglucose isomerases in *Clarkia*. Genetics 113: 101-114

Jones TWA, Gottlieb LD, Pichersky E (1986b) Reduced enzyme activity and starch level in an induced mutant of chloroplast phosphoglucose isomerase. Plant Physiol 81: 367-371

Kahana SE, Lowry OH, Schulz DW, Passoneau JV, Crawford EJ (1960) The kinetics of Phosphoglucoisomerase. J Biol Chem 235: 2178-2184

Kammerer B, Fischer K, Hilpert B, Schubert S, Gutensohn M, Weber A, Flügge UI (1998) Molecular characterization of a carbon transporter in plastids from heterotrophic tissues: the glucose 6-phosphate/phosphate antiporter. Plant Cell 10: 105-117

Kawabe A, Miyashita NT (2002) Characterization of duplicated two cytosolic phosphogluco isomerase (*PIGc*) loci in *Arabidopsis halleri* spp. *Gemmifera.* Genes Genet Syst 77: 159-165

Koch K (2004) Sucrose metabolism: regulatory mechanisms and pivotal roles in sugar sensing and plant development. Curr Opin Plant Biol 7: 235-246

Kofler H, Häusler RE, Schulz B, Groner F, Flugge UI, Weber A (2000) Molecular characterisation of a new mutant allele of the plastid phosphoglucomutase in *Arabidopsis*, and complementation of the mutant with the wild-type cDNA. Mol Gen Genet 263: 978-986

Krebs M, Held K, Binder A, Hashimoto K, Den Herder G, Parniske M, Kudla J, Schumacher K (2012) FRET-based genetically encoded sensors allow high-resolution live cell imaging of Ca^{2+} dynamics. Plant J 69: 181-192

Kruckeberg AL, Neuhaus HE, Feil R, Gottlieb LD, Stitt M (1989) Decreased-activity mutants of phosphoglucose isomerase in the cytosol and chloroplast of *Clarkia xantiana*. Impact on mass-action ratios and fluxes to sucrose and starch, and estimation of flux control coefficients and elasticity coefficients. Biochem J 261: 457-467

Kunz HH, Häusler RE, Fettke J, Herbst K, Niewiadomski P, Gierth M, Bell K, Steup M, Flugge UI, Schneider A (2010) The role of plastidial glucose-6-phosphate/phosphate translocators in vegetative tissues of *Arabidopsis thaliana* mutants impaired in starch biosynthesis. Plant Biol 12: 115-128

Lee BT, Matheson NK (1984) Phosphomannoisomerase and phosphoglucoisomerase in seeds of *Cassia coluteoides* and some other legumes that synthesize galactomannan. Phytochem 23: 983-987

Levy YY, Dean C (1998) The transition to flowering. Plant Cell 10: 1973-1989

Lin TP, Caspar T, Somerville C, Preiss J (1988) Isolation and characterization of a starchless mutant of *Arabidopsis thaliana* (L.) Heynh lacking ADP-glucose pyrophosphorylase activity. Plant Physiol 86: 1131-1135

Liu J, Vance CP (2010) Crucial roles of sucrose and microRNA399 in systemic signaling of P deficiency; A tale of two team players? Plant Signal Behav 5: 1556-1560

Lloyd JR, Kossmann J, Ritte G (2005) Leaf starch degradation comes out of the shadows. Trends Plant Sci 10: 130-137

Lu Y, Sharkey TD (2004) The role of amylomaltase in maltose metabolism in the cytosol of photosynthetic cells. Planta 218: 466-473

Lu Y, Gehan JP, Sharkey TD (2005) Day length and circadian effects on starch degradation and maltose metabolism. Plant Physiol 138: 2280-2291

Lu Y, Steichen JM, Yao J, Sharkey TD (2006) The role of cytosolic a-glucan phosphorylase in maltose metabolism and the comparison of amylomaltase in *Arabidopsis* and *Escherichia coli*. Plant Physiol 142: 878-889

Ludewig F, Flügge UI (2013) Role of metabolite transporters in source-sink carbon allocation. Front Plant Sci 4: 231-doi: 103389/fpls.2013.00231

Malinova I, Steup M, Fettke J (2013) Carbon transitions from either Calvin cycle or transitory starch to heteroglycans as revealed by ^{14}C-labeling experiments using protoplasts from *Arabidopsis*. Physiol Plant 149: 25-44

Maxwell K, Johnson GN (2000) Chlorophyll fluorescence--a practical guide. J Exp Bot 51: 659-668

Meinke DW, Sussex IM (1979) Embryo-Lethal Mutants of Arabidopsis thaliana; A model system for genetic analyses of plant embryo development. Dev Biol 72: 50-61

Nagaya S, Kawamura K, Shinmyo A, Kato K (2010) The HSP terminator of *Arabidopsis thaliana* increases gene expression in plant cells. Plant Cell Physiol 51: 328-332

Nakagawa T, Kurose T, Hino T, Tanaka K, Kawamukai M, Niwa Y, Toyooka K, Matsuoka K, Jinbo T, Kimura T (2007) Development of series of gateway binary vectors, pGWBs, for realizing efficient construction of fusion genes for plant transformation. J Biosci Bioeng 104: 34-41

Neuhaus HE, Kruckeberg AL, Feil R, Stitt M (1989) Reduced-activity mutants of phosphoglucose isomerase in the cytosol and chloroplast of *Clarkia xantiana*. Planta 178: 110-122

Niewiadomski P, Knappe S, Geimer S, Fischer K, Schulz B, Unte US, Rosso MG, Ache P, Flügge UI, Schneider A (2005) The *Arabidopsis* plastidic glucose 6-phosphate/phosphate translocator GPT1 is essential for pollen maturation and embryo sac development. Plant Cell 17: 760-775

Niittylä T, Messerli G, Trevisan M, Chen J, Smith AM, Zeeman SC (2004) A previously unknown maltose transporter essential for starch degradation in leaves. Science 303: 87-89

Norris SR, Meyer SE, Callis J (1993) The intron of *Arabidopsis thaliana* polyubiquitin genes is conserved in location and is a quantitative determinant of chimeric gene expression. Plant Mol Biol 21: 895-906

Park SK, Howden R, Twell D (1998) The Arabidopsis thaliana gametophytic mutation gemini pollen1disrupts microspore polarity, division asymmetry and pollen cell fate. Development 125: 3789-3799

Patrick JW, Botha F, Birch RG (2013) Metabolic engineering of sugars and simple sugar derivatives in plants. Plant Biotech J 11: 142-156

Pleite R, Pike MJ, Garses R, Martinez-Force E, Rawsthorne S (2005) The sources of carbon and reducing power for fatty acid synthesis in the heterotrophic plastids of developing sunflower (Helianthus annuus L.) embryos. Plant J 53: 1297-1303

Pracharoenwattana I, Zhou W, Keech O, Francisco PB, Udomchalothorn T, Tschoep H, Stitt M, Gibon Y, Smith SM (2010) *Arabidopsis* has a cytosolic fumarase required for the massive allocation of photosynthate into fumaric acid and for rapid plant growth on high nitrogen. Plant J 62: 785-795

Pressman E, Shaked R, Shen S, Altahan L, Firon N (2012) Variations in carbohydrate content and sucrose-metabolizing enzymes in tomato (*Solanum lycopersicum* L.) stamen parts during pollen maturation. Am J Plant Sci 3: 252-260

Procissi A, de Laissardière S, Férault M, Vezon D, Pelletier G, Bonhomme S (2001) Five gametophytic mutations affecting pollen development and pollen tube growth in Arabidopsis thaliana. Genetics 158: 1773-1783

Quettier AL, Shaw E, Eastmond PJ (2008) SUGAR-DEPENDENT6 encodes a mitochondrial flavin adenine dinucleotide-dependent glycerol-3-p dehydrogenase, which is required for glycerol catabolism and postgerminative seedling growth in Arabidopsis. Plant Physiol 148: 519-528

Rasse DP, Tocquin P (2006) Leaf carbohydrate controls over *Arabidopsis* growth and response to elevated CO2: an experimentally based model. New Phytol 172: 500-513

Riou-Khamlichi C, Menges M, Healy JMS, Murray JAH (2000) Sugar control of the plant cell cycle: differential regulation of *Arabidopsis* D-type cyclin gene expression. Mol Cell Biol 20: 4513-4521

Rounds CM, Winship LJ, Hepler PK (2011) Pollen tube energetics: respiration, fermentation and the race to the ovule. AoB Plants 2011: doi: 10.1093/aobpla/plr019

Sanders PM , Bui AQ, Weterings K, McIntire KN , Hsu YC, Lee PY, Truong MT, Beals TP, Goldberg RB (1999) Anther developmental defects in Arabidopsis thaliana male-sterile mutants. Sex Plant Reprod 11: 297-322

Sangwan RS, Singh R (1989) Characterization of cytosolic phosphoglucoisomerase from immature wheat (*Triticum aestivum* L.) endosperm. J Biosci 14: 47-54

Scialdone A, Mugford ST, Feike D, Skeffington A, Borrill P; Graf A, Smith AM, Howard M (2013) Arabidopsis plants perform arithmetic division to prevent starvation at night. eLife 2: 1-24

Seaton DD, Ebenhöh O, Millar AJ; Pokhilko A (2014) Regulatory principles and experimental approaches to the circadian control of starch turnover. J Royal Soc Interface 11: 20130979

Sicher R (2011) Carbon partitioning and the impact of starch deficiency on the initial response of Arabidopsis to chilling temperatures. Plant Sci 181: 167-176

Schnarrenberger C, Oeser A (1974) Two isoenzymes of glucosephosphate isomerase from spinach leaves and their intracellular compartmentation. Eur J Biochem 45: 77-82

Schneider A, Häusler RE, Kolukisaoglu U, Kunze R, van der GE, Schwacke R, Catoni E, Desimone M, Flugge UI (2002) An *Arabidopsis thaliana* knock-out mutant of the chloroplast triose phosphate/phosphate translocator is severely compromised only when starch synthesis, but not starch mobilisation is abolished. Plant J 32: 685-699

Schreiber U, Schliwa U, Bilger W (1986) Continuous recording of photochemical and non-photochemical chlorophyll fluorescence quenching with a new type of modulation fluorometer. Photosyn Res 10: 51-62

Schwab R, Ossowski S, Riester M, Warthmann N, Weigel D (2006) Highly specific gene silencing by artificial microRNAs in *Arabidopsis*. Plant Cell 18: 1121-1133

Schwacke R, Schneider A, van der Graaff E, Fischer K, Catoni E, Desimone M, Frommer WB, Flügge UI, Kunze R (2003) ARAMEMNON, a novel database for *Arabidopsis* integral membrane proteins. Plant Physiol 131: 16-26

Sharkey TD, Savitch LV, Vanderveer PJ, Micallef BJ (1992) Carbon partitioning in a *Flaveria linearis* mutant with reduced cytosolic fructose bisphosphatase. Plant Physiol 100: 210-215

Smith AM, Zeeman SC, Smith SM (2005) Starch degradation. Annu Rev Plant Biol 56:73-98

Srivastava AC, Ganesan S, Ismail IO, Ayre BG (2008) Functional characterization of the *Arabidopsis* AtSUC2 sucrose/H^+ symporter by tissue-specific complementation reveals an essential role in phloem loading but not in long-distance transport. Plant Physiol 148: 200-211

Stitt M (1986) Limitation of photosynthesis by carbon metabolism: I. Evidence for excess electron transport capacity in leaves carrying out photosynthesis in saturating light and CO_2. Plant Physiol 81: 1115-1122

Stitt M (1990) Fructose 2,6-bisphosphate as a regulatory molecule in plants. Annu Rev Plant Physiol Plant Mol Biol 41: 153-185

Stitt M (1996) Metabolic regulation of photosynthesis. *In:* Advances in Photosynthesis. Environmental Stress and Photosynthesis (Baker N, ed.). London: Academic Press 3: 151-190

Stitt M, Huber SC, Kerr P (1987) Control of photosynthetic sucrose synthesis. In: Biochemistry of Plants (Hatch MD. & Boardman NK eds). London: Academic Press 10: 327-409

Stitt M, Wirtz W, Gerhardt R, Heldt HW, Spencer C, Walker D, Foyer C (1985) A comparative study of metabolite levels in plant leaf material in the dark. Planta 166: 354-364

Stitt M, Zeeman SC (2012) Starch turnover: pathways, regulation and role in growth. Curr Opin Plant Biol 15: 282-292

Strand A, Zrenner R, Trevanion S, Stitt M, Gustafsson P, Gardeström P (2000) Decreased expression of two key enzymes in the sucrose biosynthesis pathway, cytosolic fructose 1,6-bisphosphatase and sucrose phosphate synthase, has remarkably different consequences for photosynthetic carbon metabolism in transgenic *Arabidopsis thaliana.* Plant J 23: 759-770

Streb S, Eicke S, Zeeman SC (2012) The simultaneous abolition of three starch hydrolases blocks transient starch breakdown in *Arabidopsis*. J Biol Chem 287: 41745-41756

Sulpice R, Flis A, Ivakov AA, Apelt F, Krohn N, Encke B, Abel C, Feil R, Lunn JE, Stitt M (2014) *Arabidopsis* coordinates the diurnal regulation of carbon allocation and growth across a wide range of photoperiods. Mol Plant 7: 137-155

Thomas BR, Ford VS, Pichersky E, Gottlieb LD (1993) Molecular characterization of duplicate cytosolic phosphoglucose isomerase genes in clarkia and comparison to the single gene in Arabidopsis. Genetics 135: 895-905

Thushani RP, Xu XM, Zhao Q, Wang HJ; Meier I (2011) RanGAP is required for post-meiotic mitosis in female gametophyte development in Arabidopsis thaliana. J Exp Bot 62: 2705-2714

Tripathi SM, Singh KP (2008) Abnormal anther development and high sporopollenin synthesis in benzotrialoze treated male strile *Helianthus annuus* L. Indian J Exp Biol 46: 71-78

Troncoso-Ponce MA, Rivoal J, Cejudo FJ, Dorion S, Garces R, Martınez-Force E (2010) Cloning, biochemical characterisation, tissue localization and possible post-translational regulatory mechanism of the cytosolic phosphoglucose isomerase from developing sunflower seeds. Planta 232: 845-859

Usadel B, Blasing OE, Gibon Y, Retzlaff K, Hoehne M, Gunther M, Stitt M (2008) Global transcript levels respond to small changes of the carbon status during progressive exhaustion of carbohydrates in *Arabidopsis* rosettes. Plant Physiol 146: 1834-1861

Vosloh D (2011) Subcellular compartmentation of primary carbon metabolism in mesophyll cells of *Arabidopsis thaliana*. Dissertation, MPI for molecular physiology, University of Potsdam, Germany

Walters RG, Ibrahim DG, Horton P, Kruger NJ (2004) A mutant of Arabidopsis lacking the triose-phosphate/phosphate translocator reveals metabolic regulation of starch breakdown in the light. Plant Physiol 135: 891-906

Weber A, Servaites JC, Geiger DR, Kofler H, Hille D, Groner F, Hebbeker U, Flügge UI (2000) Identification, purification, and molecular cloning of a putative plastidic glucose translocator. Plant Cell 12: 787-802

Weeden NF, Gottlieb LD (1982) Dissociation, reassociation and purification of plastid and cytosolic phosphoglucose isomerase isozymes. Plant Physiol 69: 717-723

Weise SE, Weber AP, Sharkey TD (2004) Maltose is the major form of carbon exported from the chloroplast at night. Planta 218: 474-482

Winter D, Vinegar B, Nahal H, Ammar R, Wilson GV, Provart NJ (2007) An "Electronic Fluorescent Pictograph" Browser for Exploring and Analyzing Large-Scale Biological Data Sets. Plos One 2: e718-doi:10.1371/journal.pone.0000718

Yazdanbakhsh N, Sulpice R, Graf A, Stitt M, Fisahn J (2011) Circadian control of root elongation and C partitioning in *Arabidopsis thaliana*. Plant Cell Environ 34: 877-894

Yu TS, Lue WL, Wang SM, Chen J (2000) Mutation of *Arabidopsis* plastid phosphoglucose isomerase affects leaf starch synthesis and floral initiation. Plant Physiol 123: 319-326

Zeeman S, Smith SM, Smith AM (2004) The breakdown of starch in leaves. New Phytol 163: 247-261

Zeeman SC, Smith SM, Smith AM (2007) The diurnal metabolism of leaf starch. Biochem J 401: 13-28

Zhou R, Cheng L (2008) Competitive inhibition of phosphoglucose isomerase of apple leaves by sorbitol 6-phosphate. Plant Physiol 165: 903-910

Zrenner R, Krause KP, Apel P, Sonnewald U (1996) Reduction of the cytosolic fructose 1,6-bisphosphatase in transgenic potato plants limits photosynthetic sucrose biosynthesis with no impact on plant growth and tuber yield. Plant J 9: 671- 681

Abstract

Phosphoglucoisomerase (PGI) is a key enzyme in carbohydrate metabolism. Two copies of this enzyme are encoded in the genome of *Arabidopsis thaliana*, one of which is located in plastids and the other one in the cytosol. Since loss-of-function of the plastidic isoform (*PGI1*) has already been analyzed and mutants have been shown to be starch-free, we were interested in the characterization of the cytosolic isoform (*cPGI*), which is involved in sucrose production.

Absence of homozygous T-DNA mutants from the progeny of heterozygous parent plants and decreased transmission efficiency of the mutant allele through male and female gametes indicated impairment of both gametophyte and embryo vitality and development. Since homozygous T-DNA mutants were not available, we employed an artificial micro RNA (amiRNA)-based approach. For this purpose, two independent amiRNAs (1 and 2) against the *cPGI* mRNA were designed and two lines (*6* and *10*) from amiR1-*cpgi* and three lines (*8*, *9* and *10*) from amiR2-*cpgi* were chosen for further analyses. Although cPGI activity was completely lost, these plants were viable but reduced in growth, leaf area and fresh weight compared to the wild-type.

Furthermore, amiR-*cpgi* plants showed starch excess in chloroplasts and decreased sucrose content in leaves at the end of the night and an increased glucose content of cytosolic heteroglycans. In addition, simultaneous loss of cPGI activity and the ability to generate transitory starch led to severely impaired plant growth that could only be complemented by provision of external sucrose. These data suggest that amiR-*cpgi* plants may compensate loss of cPGI activity by partial starch degradation during the day which would provide an alternative source of glucose-6-phosphate necessary for sucrose production during the day. Moreover, photosynthesis in amiR-*cpgi* plants was impaired with plants displaying increased non-photochemical quenching (NPQ) in mutant plants making them easily distinguishable from the wild-type (Col-0).

Taken together, results show that loss of *cPGI* function in mature leaves of amiR-*cpgi* mutants can be tolerated by the plant but strongly affects nocturnal starch breakdown and impacts the photosynthetic apparatus. However, during gametophyte and embryo development loss of *cPGI* function can apparently not be compensated metabolically, since viable homozygous T-DNA mutants could not be identified.

Zusammenfassung

Die Phosphoglucoisomerase (PGI) ist ein Schlüsselenzym des Kohlenhydratstoffwechsels. Im Genom der Ackerschmalwand *Arabidopsis thaliana* sind zwei Isoformen dieses Enzyms kodiert, wobei eine im Plastiden und die andere im Zytosol lokalisiert ist. Der Verlust der plastidären Isoform PGI1 führt zu einem vollständigen Ausfall des Stärkeaufbaus in der Pflanze, wie vorangegangene Untersuchungen an der PGI1-defizienten Mutante zeigen konnten. Die aktuelle Arbeit jedoch legt ihren Fokus auf die Charakterisierung der cytosolischen Isoform (*cPGI*), welche in der Saccharose-Biosynthese involviert ist.

In der Nachkommenschaft heterozygoter *cpgi* T-DNA Insertionsmutanten konnten keine homozygoten Individuen nachgewiesen werden. In Verbindung mit einer reduzierten Transmissionseffizienz des Mutantenallels durch männliche und weibliche Gameten weist dies auf eine beeinträchtigte Gametophyten- und Embryonenvitalität und -entwicklung hin. In Ermangelung homozygoter T-DNA-Linien wurde ein microRNA (amiRNA)-basierter Ansatz verfolgt. Hierzu wurden zwei unabhängige amiRNAs gegen die *cPGI* mRNA (amiR1-*cpgi* und amiR2-*cpgi*) hergestellt und für die anschließenden Analysen zwei Linien der amiR1-*cpgi* (*6* und *10*) und drei Linien der amiR2-*cpgi* (*8*, *9* und *10*) ausgewählt. Trotz des vollständigen Verlustes der cPGI-Aktivität waren die Pflanzen lebensfähig, jedoch wiesen sie im Vergleich zum Wildtyp ein reduziertes Wachstum, sowie verringerte Blattflächen und Frischgewichte auf.

Weiterhin zeichneten sich amiR-*cpgi* Pflanzen durch eine Stärke Überakkumulation in Chloroplasten und einen reduzierten Saccharose-Gehalt in Blättern am Ende der Nacht aus, sowie durch einen erhöhten Glukosegehalt der cytosolischen Heteroglukane. Darüber hinaus führt der gleichzeitige Verlust von cPGI-Aktivität und der Fähigkeit transitorische Stärke zu bilden zu einer massiven Reduktion des Pflanzenwachstums, was nur durch die Gabe externer Saccharose kompensiert werden konnte. Diese Daten legen den Schluss nahe, dass amiR-*cpgi* Pflanzen den Verlust an cPGI Aktivität durch partiellen Stärkeabbau während des Tages kompensieren können und sich dadurch eine alternative Quelle für Fruktose-6-Phosphat zur Saccharosesynthese erschließen. Außerdem ist auch die Fotosynthese in amiR-*cpgi* Pflanzen beeinträchtigt. amiR-*cpgi* Pflanzen zeigen ein

erhöhtes nicht-photochemisches Quenching (NPQ), was es möglich macht, amiR-*cpgi* Pflanzen leicht von Wildtyppflanzen (Col-0) zu unterscheiden.

Zusammenfassend lässt sich sagen, dass der Verlust der *cPGI* Funktion in ausgewachsenen Blättern von amiR-*cpgi* Mutanten durch die Pflanze zwar toleriert werden kann, jedoch einen starken Effekt auf den nächtlichen Stärkeabbau hat und eine Beeinträchtigungen des Fotosynthese-Apparates bedingt. Während der Gametophyten- und Embryoentwicklung jedoch scheint dieser Verlust nicht metabolisch kompensierbar zu sein, da lebensfähige, homozygote T-DNA-Mutanten nicht identifiziert werden konnten.

Acknowledgement

First of all, I am deeply grateful to Prof. Dr. Ulf-Ingo Flügge who gave me the unique opportunity to work in his lab and gave me a great support in the past years.

Many thanks to Prof. Dr. Stanislav Kopriva and Prof. Dr. Karin Schnetz for kindly agreeing to participate in the referee committee.

Foremost, I would like to express my gratitude to Dr. Markus Gierth for his patience, thoughtfulness, motivation and kindness. Thank you so much for the great scientific advices and unforgettable supervision.

I would like to gratefully thank Dr. Henning Kunz who initiated this project and whom I have been inspired by his integrity and devotion to science.

I am grateful to Dr. Olof Persson and Dr. Isabell Witt for their nice coordination and guidance over these three years.

My sincere thanks also go to PD. Dr. Jörg Fettke and Dr. Irina Malinova from University of Potsdam for a nice collaboration and measurement of soluble heterogylcan.

A great appreciation goes to Sonja Lott, not only for her technical assistance but rather for her sisterhood. I loved each single of moments of life advice, daily talk and working together in the lab.

I would like to thank Dr. Katja Ludewig and Dr. Stephan Krüger for nice discussion, helps, guidance, decision making and to become really good friends of mine.

My special thanks go to Dr. Frank Ludewig, Dr. Rainer E. Häusler and Dr. Tamara Gigolashvili for their constructive suggestions and helpful comments.#

I would also like to thank my wonderful fellow lab-mates and friends; Dr. Anke Kuhn, Elke Hilgers, Sabine Wulfert, Dr. Veronika Schneck, Raphael Wemhöner, Dr. Simon von Berlepsch, Nicole Wöstefeld, Laura Strubl, Daniela Mertens, Ruben M. Benstein, Luisa Heinrichs, Natallia Ashykhmina#and all AG Flügge for always being there in needs and for all those memorable moments we have made together.

Finally, I am pleased of having the greatest parents on whose shoulders I have been placed now. I give you my heartful thanks for any moments of inspiration you have been giving me in life. My deep love also goes to my sisters Nazanin and Negar whom acted as wonderful role models in supporting, loving, caring and educational paths of their little sis!

I will never forget how grateful I am to all of you.

Shirin Zamani-Nour
June 2014

Erklärung

Ich versichere, dass ich die von mir vorgelegte Dissertation selbständig angefertigt, die benutzten Quellen und Hilfsmittel vollständig angegeben und die Stellen der Arbeit- einschließlich Tabellen, Karten und Abbildungen -, die anderen Werken im Wortlaut oder dem Sinn nach entnommen sind, in jedem Einzelfall als Entlehnung kenntlich gemacht habe; dass diese Dissertation noch keiner anderen Fakultät oder Universität zur Prüfung vorgelegen hat; dass sie - abgesehen von unten angegebenen Teilpublikationen - noch nicht veröffentlicht worden ist sowie, dass ich eine solche Veröffentlichung vor Abschluss des Promotionsverfahrens nicht vornehmen werde. Die Bestimmungen der Promotionsordnung sind mir bekannt. Die von mir vorgelegte Dissertation ist von Prof. Dr. Ulf-Ingo Flügge betreut worden.

Shirin Zamani-Nour